Metalloprotease Gp63 targeting novel glycoside exhibits potential antileishmanial activity

Amrita Chakrabarti[1§], Chintam Narayana[2§], Nishant Joshi[1], Swati Garg[5], Lalit Garg[3], Ram Sagar[2,4*], Soumya Pati[1*], Shailja Singh[1,5 *]

[1]*Department of Life Sciences, School of Natural Sciences, Shiv Nadar University, Uttar Pradesh 201314, India*

[2]*Department of Chemistry, School of Natural Sciences, Shiv Nadar University, Uttar Pradesh 201314, India*

[3]*Gene Regulation Laboratory, National Institute of Immunology, New Delhi, India*

[4]*Department of Chemistry, Institute of Science, Banaras Hindu University, Varanasi 221005, Uttar Pradesh, India*

[5]*Special Centre for Molecular Medicine, Jawaharlal Nehru University, New Delhi, India*

[*]*Email: shailja.jnu@gmail.com, soumya.pati@snu.edu.in, , ram.sagar@bhu.ac.in,*

§ These authors contributed equally to this work.

Highlights

- **A novel glycoside derivative (Gly 2) targets Gp63 functioning in *L. donovani* promastigotes, resulting in its abrogated proliferation and severely detabilized redox homeostasis, leading to parasitic death.**
- **Structure activity relationship (SAR) analysis revealed exceptional ligandability of Gly 2 towards Gp63 catalytic domain both *in silico* and in Cellular Thermal Shift Assay (CETSA) based *in vitro* analysis.**
- **Gly 2 treatment exhibited increased parasite susceptibility towards complement mediated lysis and reduced macrophage infection *in vitro* mimicking the pathophysiological conditions.**
- **Gly 2 showed profound antileishmanial activity against the clinical isolates of Post Kala-azar Dermal Leishmaniasis (PKDL).**

Abstract

Visceral Leishmaniasis (VL) and its aggressive cutaneous exacerbation known as Post Kala-azar Dermal Leishmaniasis (PKDL) cause a huge disease burden in tropics and sub-tropic endemic zones worldwide. Contemporary treatment modalities have been associated with various complications. Encouraged from the recent marked antimalarial effects from plant derived glycosides; here we have chemically synthesized a library of diverse Glycoside derivatives (Gly 1-12) and evaluated their inhibitory efficacy against *Ag83* strain of *Leishmania donovani. In vitro* activity of Glycoside-2 **(Gly 2)** on promastigote form of *Ag83* strain, unravelled its prominent anti-leishmanial property with **IC50** value of 1.13µM. *In-silico* studies also unveiled the efficacy of **Gly 2** to bind to the membrane surface of parasite. The toxic effect of **Gly 2** causes necrosis like death in promastigote by abrogating its proliferation leading to imbalanced redox homeostasis by disruption of mitochondrial membrane potential. Additionally, **Gly 2** treatment demonstrated increased susceptibility of parasites towards complement mediated lysis and displayed strong lethal effect on amastigote-macrophage infection model mimicking pathophysiological condition of body. This lead molecule was quite effective against the clinical on promastigotes form of PKDL strain BS12 with IC50 value of 1.97 µM making it the most suitable drug so far which can target both VL and PKDL simultaneously. Based on the above experimental validations we narrowed our thoughts regarding the potent role of **Gly 2** targeting surface protein of *L. donovani* such as Gp63, a zinc metalloprotease. Further analysis of structure activity relationship (SAR) of these glycoside derivatives, demonstrated exceptional binding affinity of **Gly 2** towards Gp63, a zinc metalloprotease of *L. donovani*; with strong H-bond interactions of **Gly 2** with catalytic domain in the α-helix B region of Gp63. The strong confined interactions between **Gly 2** and the target protein Gp63 in a physiologically relevant cellular environment was further assessed by Cellular Thermal Shift Assay **(CETSA)** which corroborated with our previous results. Taken together, this study reports the serendipitous discovery of glycoside derivative **Gly 2** with enhanced leishmanicidal activity and proves to be novel chemotherapeutic prototype against VL and PKDL.

Keywords: Leishmania, Glycoside 2, LdGp63, CETSA

1. Introduction

Leishmaniasis is a globally neglected vector-borne disease, transmitted by the bite of female sand fly infected with the protozoan parasite of genus *Leishmania*. It has a diverse range of clinical manifestations ranging from a mild cutaneous variant to the life-threatening visceral form [1]. Those patients who are apparently cured of Visceral Leishmaniasis (VL), are prone to Post kala-azar dermal leishmaniasis (PKDL), an aggressive clinical manifestation of VL [2]. Kala-azar is caused by *L. donovani* which is endemic to several parts of the tropics, subtropics, and southern Europe; is a severe threaten to 350 million people, with a prevalence of 12 million people worldwide [3]. In addition to it, an estimated 0·7–1 million newly reported cases of leishmaniasis erupt out every year [4]. Thus, targeting the fatal disease; WHO has already declared the development of new treatments with utmost priority.

Over several years, the available diagnosis and treatment modalities for VL relied on pentavalent antimonials using compounds like sodium stibogluconate and meglumine antimoniate. But they are found to be unsatisfactory in combating the alarming situation of arising new cases leading to sudden increase in disease burden. The underlying barricades towards their failure were high toxicity, delayed drug release and response; inimical side effects and development of resistance towards the available drug regimen [5] [6]. One of the contemporary approaches includes the use of amphotericin B accompanied by emanation of miltefosine as the first oral drug therapy for VL [7]. In the conquest for identifying better leishmanicidal compounds, plant-derived and/or mimicking products have been gaining ground. This includes Aloe vera, luteolin, quassin, berberine chloride and artemisinin among others [8] which share a common mode of action; inducing oxidative stress leading to parasite death. But they too depicted certain side-effects and low efficacy. Thus, briefly current armamentarium of anti-leishmanial drugs is far from satisfactory [9].

This demands the very requirement for effective drug discovery and development approach based on enzyme linked target identification; corresponding molecular pathway and cellular homeostasis of parasite involved in VL. Previous studies elucidated the role of various *Leishmania spp.* proteases involved in life cycle and pathogenesis of the parasite [10]. Among them zinc metalloprotease, Gp63

83 or leishmanolysin of *Leishmania spp.* have been identified as an important multifunctional virulence
84 factor, found in abundance on the surface of *Leishmania spp.* promastigotes. It is also present in limited
85 quantities inside the parasite [11] [12]. It is the key enzyme responsible for parasite propagation,
86 promastigote binding to and internalization in macrophages as well as attenuation of formation of
87 reactive oxygen intermediates favouring amastigote proliferation [13]. The myriad diversity as well as
88 the high catalytic activity at body's physiological temperature of this virulence factor favours the
89 dissemination of the parasite in host [14] [15] [11] [16]. Apart from its major role in maintaining cellular
90 homeostasis in parasite survival, recent experiments performed using discreet parasitic models
91 demonstrated the protective nature of Gp63 against complement fixation and processing, which shields
92 *Leishmania* promastigotes during its tarriance into mammalian hosts [17] [18] [19].

93 Considering the above scenario, we have designed a library of novel glycoside derivatives with D-
94 glucose and N-acetyl-D-glucosamine as primary backbone template. We have used green chemistry
95 approach which is a forward, unidirectional, single step synthesis process with no toxic byproducts and
96 an unbiased method for designing target molecules [20]. Due to their volatile abundance in nature and
97 relatively simpler conformation; glycoside derivatives are gaining current momentum as bioactive
98 molecules in pharmaceutical industries [21].

99 These molecules were found to be completely non-toxic in mammalian cells and the hits showed
100 promising result against both forms of *L. donovani* promastigotes as well as intra-macrophagic
101 amastigotes. The Glycoside 2 **(Gly 2)** showed strong potency against lab and clinical strains of *L.*
102 *donovani* at 1.13μM and 1.6μM (=IC50) concentration respectively, while mammalian cells were
103 tolerant to the presence of **Gly 2** in mM range. **Gly 2** treatment leads to abrogation of parasite
104 multiplication, induction of ROS generation and disruption of mitochondrial membrane potential
105 leading to promastigote death. Besides its inhibitory role in *in-vitro* cultured parasites we have
106 demonstrated its efficacy in body's physiological condition where it marked prevention of parasite
107 evasion from complement mediated lysis. Additionally, **Gly 2** was quite effective against the BS12, a
108 clinical isolate of PKDL. Thus, owing to these observations, we evaluated the structure activity
109 relationship (SAR) of the novel glycosides having hydrophilic head group and variable chain length of

110 tail (lipophilic group). It helps to screen a large number of molecules spanning distinct regions of the
111 bioactive chemical space; which is an inherent property seen in natural products [22]. We have
112 demonstrated efficient binding of **Gly 2** molecule with Gp63 using Cellular Thermal Shift Assay
113 (CETSA) and *in silico* studies. Furthermore, **Gly 2** displayed exemplary lethal effect on amastigote
114 stage of parasite and found to be efficient enough in pathogen clearance within a macrophage infection
115 model at 3.5µM (≥IC50). Additionally, **Gly 2** could target both VL and PKDL simultaneously. Thus,
116 **Gly 2** not only proves to be absolute benign to mammalian cells but it also subverts the parasite
117 mechanism of immune evasion making it as a potent antileishmanial against VL and PKDL.

118 **2. Materials and methods**

119 **2.1 Parasite growth and maintenance**

120 Promastigote-forms of *L. donovani* (Ag83 strain) were cultured at 26 ºC in M199 media (GIBCO,
121 India), pH 7.4 supplemented with 10% (v/v) inactivated Fetal Bovine Serum (FBS, GIBCO, India) and
122 0.02 mg/mL gentamycin (Life Technologies, USA**).** The clinical isolate of PKDL, BS12 was a gift from
123 Prof. Mitali Chatterjee Lab (Institute of post graduate medical research, India). These isolates were
124 routinely cultured at 22°C in M199 medium (GIBCO, India) with 100 U/mL penicillin-streptomycin
125 (Gibco, Invitrogen, Thermo Fisher Scientific, NY), 8 µM hemin (4 mM stock made in 50%
126 triethanolamine) (Sigma, USA), 25mM Hepes (N-[2-hydroxyethyl]piperazine-N0-[2-ethanesulfonic
127 acid; Sigma]), supplemented with 10% heat inactivated FBS (GIBCO, India). Cultures were maintained
128 between 10^6 and 10^7 cells/mL for continuous exponential growth. $1X10^6$ cells /mL parasite count was
129 constantly maintained for all the experiments.

130 **2.2 Cell Culture**

131 The J774.A1 murine macrophage cells were grown in Roswell Park Memorial Institute (RPMI) 1640
132 Medium in the presence of 10% (v/v) FBS and penicillin−streptomycin (Gibco, Invitrogen, Thermo
133 Fisher Scientific, NY) at 37°C (humidified) and 5% CO_2. Primary MDCK cells were obtained from the
134 National Centre for Cell Science, Pune, India. MDCK cells were derived from the kidney tissue of an
135 adult female cocker spaniel. These were grown in Dulbecco's modified Eagle's minimal essential

136 medium (DMEM) in the presence of 10% (v/v) FBS and penicillin−streptomycin (Gibco, Invitrogen,
137 Thermo Fisher Scientific, NY) at 37°C (humidified) and 5% CO_2.

138 **2.3 General procedure for Synthesis of glycoside derivatives**

139 Pre-stirred solution of glucose (200 mg, 1.11 mmol) or glucosamine (200 mg, 1.11 mmol) was prepared
140 in neat alcohol (5-10 mL) and Amberlite IR 120-H^+ resin (400 mg) was added to it. The resulting
141 mixture was stirred at 100°C for 24 h. After completion of the reaction, the mixture was cooled down
142 to room temperature, and filtered to remove the resin. The filtrate was evaporated under reduced
143 pressure to obtain compound **1-3** as white solid in acceptable to good yield. Compounds **4-6** were
144 prepared in good yield adopting similar reaction protocol using corresponding alcohol and glucose or
145 glucosamine followed by acetylation using acetic anhydride in pyridine at room temperature. All the
146 final compounds **1-6** were purified using flash column chromatography before using them for biological
147 activity. The final compounds were formed as semi-solid or solid and were characterized by ^{1}H-NMR
148 and ^{13}C-NMR. ^{1}H-NMR and ^{13}C-NMR spectra in CD_3OD and D_2O were recorded on Bruker 400 MHz
149 spectrometer at ambient temperature.^{1}H recorded by 400 MHz and ^{13}C recorded by 100 MHz. Proton
150 chemical shifts are given in ppm relative to the internal standard (tetramethylsilane) or referenced
151 relative to the solvent residual peaks (CD3OD: δ 3.31). Multiplicity was denoted as follows: s (singlet);
152 d (doublet); t (triplet); q (quartet), m (multiplet): dd (doublet of doublet); dt (doublet of triplet); td (triplet
153 of doublet); ddd (doublet of doublet of doublet), etc. Coupling constants (J) were reported in Hz.
154 Column chromatography was performed by using silicagel 100-200 and 230-400 mesh. HRMS spectra
155 determined from quadrapole/Q-TOF mass spectrometer with an ESI source (Supplementary text 1).

156 **2.4 Treatment procedure**

157 All the compounds were dissolved in dimethyl sulphoxide (DMSO) (Sigma-Aldrich) for 1mM stock
158 solution and was screened against promastigotes at concentration of 5µM. For Glycosides (Gly) 2, 6
159 and 8 a range of concentrations starting from 100nM to 100µM were screened against promastigote
160 form of parasite and mammalian cells; 5µM was the working concentration for these Compounds
161 (>IC50 value) in all *in-vitro* experiments.

162 **2.5 Anti-parasite drug susceptibility assay**

163 Initially, promastigotes of Ag83 strain of *L. donovani* were exposed to various concentrations (100nM-
164 100 µM) of each compound in a 96-well microtiter plate (100 µL/well volume) and were incubated for
165 72 h at 26°C. Parasites treated with amphotericin B (3µg/mL) (Sigma-Aldrich) were maintained as the
166 positive control. Finally, LDH cytotoxic assay was performed as per standard protocol (CytoTox 96
167 Non-Radioactive Cytotoxicity Assay-Promega, USA). The percent cytotoxicity of test compounds was
168 calculated by normalizing with amphotericin B as 100%. Colorimetric quantification of toxicity towards
169 promastigotes upon treatment with various concentrations of the glycosides was carried out using LDH
170 assay. Further percentage growth inhibition was calculated using the formula:

171 % Growth Inhibition = Gly treated LDH activity- Spontaneous LDH activity

172 / Maximum LDH activity- Spontaneous LDH activity * 100

173 As per the formula, the spontaneous LDH Activity = activity of the untreated cells, and the maximum
174 LDH activity = activity of the amphotericin B treated cells. These values were transferred in the
175 GraphPad Prism version 8.0.1, and IC50 value for Gly 2, 6 and 8 treated was generated for Ag83 and
176 PKDL strain of *L. donovani* using sigmoidal dose-response model with nonlinear regression tool.

177 **2.6 Qualitative estimation of live /dead parasites**

178 The toxic effect of the three compounds, Gly 2, 6 and 8 on promastigotes at 5µM > IC50 concentration
179 was measured by Hoechst and PI double staining. After exposure with the compounds for 24 h, Parasites
180 were harvested, PBS washed and stained with Hoechst 33258 (1µg/ml) (Life Technologies, USA) and
181 PI (5 µg/mL) (Life Technologies, USA) followed by incubation for a period of 20min at 37°C.
182 Subsequently, cells were washed for excessive stain removal and visualized using fluorescence
183 microscope with 510–560 nm filter block for PI red fluorescence and excitation / emission spectra at
184 361/497 for Hoechst.

185 **2.7 *In-silico* studies**

186 The physicochemical properties of compounds were calculated using SwissADME [23] module
187 provided in SIB (Swiss Institute of Bioinformatics) webserver (https://www.sib.swiss). The designed

188 GLY compounds were evaluated for their ADME profile, including drug-likeness, partition coefficient,
189 solubility, and oral bioavailability parameters according to Lipinski's "rule-of-five".

190 **2.8 Antibody generation**

191 Synthetic oligonucleotides encoding the catalytic motif of LdGp63 with PstI and HindIII overhangs
192 were synthesized and ligated to PstI and HindIII digested pQELTB plasmid.[24], and transformed into
193 *E. coli* DH5α cells for propagation and into *E. coli* M15 cells for recombinant fusion protein expression.
194 *E.coli* M15 cells, containing the recombinant plasmid having the catalytic motif of LdGp63 in
195 translational fusion with *E. coli* heat labile enterotoxin B subunit, were induced with 1 mM IPTG.
196 Induction of expression with IPTG resulted in production of recombinant proteins as insoluble inclusion
197 bodies. The recombinant fusion protein was purified to near homogeneity from solubilized inclusion
198 bodies using metal affinity chromatography taking advantage of the histidine tag present at the N-
199 terminal of the fusion protein. Female BALB/c mice were immunized with the purified fusion protein
200 followed by a single booster on day 15 post immunization. Blood was obtained a week post booster
201 administration through retro-orbital plexus. Anti-fusion protein antiserum was obtained after incubating
202 the blood at RT for 1 h followed by centrifugation at 5000 rpm at 4 °C for 10 min. Antiserum thus
203 prepared was stored at -20ºC until further use.

204 **2.9 Western blot analysis**

205 Immunoblotting assay was performed using generated Mouse polyclonal anti-LdGp63 catalytic domain
206 which were used at 1:500 dilution. The whole-parasite lysates were washed twice with 0.01M PBS,
207 lysed in Lysis buffer (50mM Hepes, 150mM NaCl, 1% Triton X-100 and 1% IGEPAL, 1 mM
208 phenylmethyl sulfonyl fluoride). These were denatured at 70°C. The samples were then homogenized
209 with a 1-ml syringe and a 22-g needle before SDS-PAGE and blotting onto nitrocellulose membranes.
210 The membranes were blocked with 5% skimmed milk powder dissolved in PBS containing 0.1%
211 Tween-20.

212 **2.11 Promastigote Proliferation Assay**

213 Ag83 parasite growth and multiplication were assessed by Fluorescence Assorted Cell Sorting and
214 fluorescence microscopy with 6-Carboxyfluorescein diacetate succinimidyl ester (CFDA-SE, Life
215 Technologies, USA) as a probe. Promastigotes were washed thrice with 0.1M PBS. The cells were
216 labelled with CFDA-SE dye and were then incubated at 37°C for 10 min during which they were mixed
217 3 to 4 times properly. These cells were then resuspended in ice-cold M199 medium. Further they were
218 centrifuged at 1200g for 10 mins (4ºC) and resuspended in fresh medium. Cells were treated with the
219 Gly 2 and were analyzed through BD FACS DIVA for 3 consecutive replicates after 0, 24 h, 48 h and
220 72 h, respectively.

221 **2.12 Estimation of ROS levels**

222 The redox homeostasis of promastigotes was monitored both qualitatively and quantitively by 2-7
223 dichlorodihydro fluorescein diacetate (DCFDA) (Life Technologies, USA) staining. The untreated and
224 Gly 2 treated promastigotes (1×10^6 cells/mL) were cultured for 72 h. Following incubation, the parasites
225 were harvested, washed with 0.1M PBS and stained with H_2DCFDA (20µM) for 20min at 37°C. Excess
226 stain was removed by washing with PBS and samples were resuspended in PBS (50µL) and followed
227 by imaging. Fluorescence intensity was determined using an excitation filter at 485 nm and an emission
228 filter at 535 nm using confocal microscope (Nikon Ti eclipse, USA). The samples were also analysed
229 through BD FACS diva.

230 **2.13 Quantification of mitochondrial membrane potential**

231 Mitochondrial membrane ($\Delta\psi$m) potential was examined using 5,6-dichloro-2-[3-(5,6-dichloro-1,3-
232 diethyl-1,3-dihydro-2H-benzimidazol-2-ylidene)-1propenyl]-1,3-diethyl-,iodide (JC-1 dye) (Life
233 Technologies, USA) as a probe. Treated and untreated groups were incubated for 24 h. Cells were
234 washed with PBS, JC-1 labelled, and samples were analysed through FACS diva (Beckton-Dickinson,
235 Pharmingen). The approximate fluorescence excitation/emission maxima of 514/529 nm for monomeric
236 form and 585/590 nm for J-aggregate form were used. The labelled cells were also allowed to adhere
237 to glass slides for visualization under Fluorescence microscope (Nikon Ti eclipse, USA); excitation and
238 emission filters of TRITC and FITC were used.

239 **2.14 Detection of Complement-Mediated Cytolysis of Promastigotes by uptake of Propidium**
240 **Iodide**

241 Parasites with an optimum 10% non-heat inactivated normal human serum were incubated with Gly 2
242 at 5µM concentration for 15 min. Promastigote lysis was detected by uptake of PI, by use of a FACS
243 Diva flow cytometer (Beckton-Dickinson, Pharmingen), in accordance with the manufacturer's
244 protocol. Promastigotes were washed for excessive stain removal and filter block for PI red
245 fluorescence, 510–560 nm was used.

246 **2.15 *In-silico* membrane binding studies and docking studies**

247 Using PerMM web server for theoretical assessment of passive permeability of molecules across the
248 lipid bilayer, we checked the membrane binding studies with synthesized glucoside compounds. 3D
249 protein structure of *L. major* GP63 (PDB ID- 1lml) was obtained from Protein databank. BLASTp was
250 used for LdGp63 to achieve sequence identity with template (*L. major* leishmanolysin in complex Zinc
251 ion, 1LML). Homology modelling was further performed. RAMPAGE was utilized to obtain
252 Ramachandran plot. Chemical structures of compounds were synthesized through the ChemSketch.
253 Protein and Ligands structure were optimized using Swiss PDBviewer and ChemBioDraw ultra
254 respectively. AutodockVina and Cygwin terminal were utilized to execute the docking commands.
255 Binding site for the ligand was chosen around its catalytic domain residues. Chimera, Ligplus,
256 Discovery Studio and Pymol softwares were used for further analysis of docking results.

257 **2.16 Cellular Thermal Shift Assay**

258 For a CETSA in promastigotes, parasites were seeded in 6-well cell culture plates (1.0×10^6 cells /well)
259 and exposed to Gly 2 at the 5µM >IC50 for 24 h in the incubator. Control cells were incubated with an
260 equal volume of a vehicle. Following incubation, the parasites were washed with PBS to remove excess
261 drug and harvested in 200µL of a lysis solution [50mM Hepes, 150mM NaCl, 1% Triton X-100 and 1%
262 IGEPAL, 1 mM phenylmethyl sulfonyl fluoride]. The lysates were centrifuged at 14000g for 20 min at
263 4 °C, supernatants were transferred to new tubes. Further the protein concentration was measured using
264 the Pierce BCA protein assay kit. After preparation of lysates, 30µL (0.8 mg/ml) aliquots of the

265 supernatants were heated individually on a Thermomixer compact (Eppendorf) at different temperatures
266 for 7 min and then cooled at room temperature for 3 min. CETSA samples were separated by sodium
267 dodecyl sulfate–polyacrylamide gel electrophoresis, and immunoblotting was performed as described
268 previously using a mouse polyclonal anti-Ld gp63 catalytic domain antibody (1:500).

269 **2.18 Ethics statement**

270 Normal Human Serum (NHS) is obtained from Rotary Blood Bank, Tughlakabad, New Delhi. All
271 methods were carried out in accordance with relevant guidelines and regulations. Ethics Committees of
272 Shiv Nadar University approved all the experiments carried out with NHS. The Animal Ethics
273 Committee (IAEC Code #288/11) of the Jawaharlal Nehru University approved animal usage and
274 procedures for generation of antibody. Ethical statement towards the clinical isolate of PKDL strain is
275 available with host lab from where we have achieved the strain. The strain was cultured in BSL2 lab
276 facility under guidelines institutional biosafety committee, Shiv Nadar University.

277 **2.19 Statistical analysis.**

278 Student's t-test was performed to evaluate significant differences between treatment and control
279 samples in all the experiments performed using ANOVA test. P-value < 0.05 and <0.01 was considered
280 to be significant indicated as * and ** respectively. Results represent the mean ± SD of minimum three
281 independent experiments. Calculated IC50 value and all statistical analyses were performed by using
282 GraphPad Prism version 8.01. Intensity profile for western blots were calculated using ImageJ software.

283 **3. RESULT**

284 **3.1 Synthesis of glycoside-based compounds using a green synthetic route**

285 The commercially available D-glucose 1 and N-Acetyl-D-glucosamine 2 molecules were coupled along
286 with various short to long chain alcohols under acidic conditions, to design and synthesize glycoside-
287 derived compounds. The synthesis of ethyl Glycoside *N*-Acetyl-D-glucosamine (Glycoside-1) was
288 prepared by refluxing 1 in ethanol for 24 h in the presence of amberlite-H+ IR-120, which gave us the
289 desired product Glycoside-1 as anomeric mixture in good yield as described **[Fig. 1A]**. The process
290 does not involve any further purification and amberlite resin can be reused by activating it with 1 N

291 HCl in MeOH. In parallel, other compounds in this series Glycoside-2 to Glycoside-6 were also
292 prepared adopting similar reaction protocol (Methods), which resulted in good yields **(Table 1).**
293 Furthermore, the alkyl Glycoside of N-Acetyl-D-Glucosamine Glycoside-7 to Glycoside-12 were
294 prepared by refluxing N-Acetyl-D-Glucosamine with corresponding alkyl alcohols for 24 h in the
295 presence of amberlite-H+ 100 IR-120 resin, which gave the desired products as anomeric mixture in
296 good yield as shown **(Table 1).** Further characterizations of all 12 compounds were done using NMR
297 and quadrupole/Q-TOF mass spectrometer with an ESI source determined using HRMS spectra.
298 **(Supplementary text S1)**

299 .

300

301 **3.2 ADMET and drug-likeness evaluation**

302 SwissADME provides detail and extensive physicochemical profile, ADME, and medicinal chemistry
303 property of a compound. The partition coefficient and solubility are the two parameters which play an
304 important role in the physicochemical aspect. Based on predicted LogP value, it is concluded that all
305 designed compounds lie within the range value of 1.6 to 3.6. All the 12 compounds depict the
306 probability of a compound to be considered as drug candidate quality [25]. Even though LogP value
307 does not always correspond to certain ADME aspect, this parameter could, where in this case
308 .SwissADME LogP value was calculated from five different algorithm, therefore it is assumed that the
309 value represents real condition [23].

310 **3.3 *In-vitro* metabolic viability assay-based screening unravelled the lead glycoside derivatives**
311 **and their toxic impact on *L. donovani* promastigotes.**

312 To evaluate the cytotoxic effects of 12 compounds on *L. donovani* promastigotes, Lactate
313 Dehydrogenase Assay (LDH assay) was performed. This assay involves reduction of tetrazolium salts
314 to formazan during LDH-mediated catalysis of lactate to pyruvate, which can be detected at 490 nM.
315 Rate of formazan formation is proportional to the release of LDH through damaged cell membranes. At
316 preliminary screening, the promastigotes were incubated with 12 compounds at a single concentration

317 of 5µM respectively for a period of 72 h and the released LDH was estimated **(Supplementary Fig.**
318 **1A)**. Amphotericin B treated promastigotes were taken as positive control. Significant amount of
319 formazan was observed in **Glycoside (Gly) 2, 6** and **8** treated samples suggesting that these glycosides
320 could induce leakage of cytosolic LDH by exerting the toxicity on parasites. On incubation of
321 promastigotes with **Gly 2, 6** and **8** compounds at various concentrations, the lethal effect of **Gly 2**
322 (IC50=1.13µM) was found to be prominent than **Gly 6** (IC50=3.40µM) and **Gly 8** (IC50=1.61µM)
323 comparatively **[Fig. 1B (i-iii)].**

324 As LDH release through damaged cell directly correspond to percentage of dead cells, this was further
325 confirmed with live/dead dual staining of treated parasites with Hoechst and Propidium Iodide (PI)
326 dyes. To achieve this, we treated promastigotes for a period of 72 h with **Gly 2, 6** and **8** and performed
327 Hoechst/PI staining for fluorescent microscopy-based analysis. The results revealed that **[Fig. 1C]**
328 untreated promastigotes showed viability (Hoechst+/PI-) whereas the treated parasites showed cellular
329 death (Hoechst-/PI+). Ratio in the graph delineated the percentage viable/ dead parasites. Precisely, we
330 found ~89.66% Gly2 treated parasites were dead as compared to ~70% and 75% in Gly 6 and Gly 8
331 treated promastigotes respectively **[Fig. 1C (i-ii)]**. We hardly found population of dead parasites in
332 control **[Fig. 1C-i]**.

333 **3.4 *In-silico* membrane permeability study revealed varied affinity of lead glycosides towards**
334 **plasma membrane**

335 Using Permeability of Molecules across Membranes (PerMM) server and database, we evaluated the
336 passive permeability of small molecules across the lipid bilayer *in-silico.* We found that **Gly 2** was
337 impermeable to the plasma membrane with log of permeability coefficient of -9.3 at temperature 310K
338 and neutral pH of 7. On the other hand, **Gly 6** was permeable to plasma membrane with log of
339 permeability coefficient of -1.3. In comparison of **Gly 2**, **Gly 8** was partially impermeable to membrane
340 with log of permeability coefficient of -6.9. Further using GLMol the interactive 3D images of a
341 compound moving across the membrane has been visualized **[Fig. 1D]**. This strengthened our
342 hypothesis regarding probable interaction of **Gly 2** with membrane protein of parasite leading to suitable
343 target identification. To evaluate this, we later performed *in-silico* docking studies with glycosides.

344 **3.5 Lead Glycoside derivative (Gly 2) demonstrated minimal cytotoxicity in MDCK epithelial cells**
345 **and J774A.1 macrophage.**

346 Minimum level of cytotoxicity could be detected for the compound in MDCK cells as well as
347 macrophage cells. The CC50 values of **Gly 2** analogue was in the micromolar range. The selectivity
348 index (SI) for the compound was calculated as the ratio between cytotoxicity (CC50) and activity (IC50)
349 against promastigotes. The SI value for **Gly 2** were more than 1000 suggesting that the analogues are
350 at least 1000 times more specific to parasites than host cells **(Supplementary Fig. 1C, D; Table 2).**

351 **3.6 Generation of LdGp63 catalytic domain specific antibody**

352 With the help of *In-silico* studies we found the amino acid residues involved in catalytic activity of
353 Gp63 that pertaining to the catalytic domain (216-229 aa). Based on this, peptide containing catalytic
354 domain was chemically synthesized which was tagged with LTB to increase the immunogenicity in
355 mice. It was further injected in mice to develop polyclonal anti-LdGp63 antibody.

356 **3.7 Treatment with Gly 2 abrogates promastigote proliferation**

357 To further validate whether **Gly 2** treatment effectively hampers promastigotes multiplication or not;
358 we assessed the proliferation of promastigotes by quantifying the release of cell permeable dye, CFDA-
359 SE during cell division. This dye enters cells by simple diffusion, following cleavage by intracellular
360 esterase enzymes to form reactive amine products, which covalently binds to
361 intracellular lysine residues and other amine sources, producing detectable fluorescence. Decrease in
362 fluorescence intensity is proportional to generation of promastigote daughter [26]. It was observed that
363 the percentage of CFDA positive cells remained unchanged at both 24 h (81.59%), 48 h (74.68%) and
364 72 h (68.48%) at 5µM concentration of **Gly 2**, suggesting absence of cell division in the parental cell.
365 However, the untreated promastigotes showed a reduced CFDA positivity 24 h, 48 h and 72 h
366 suggesting cellular progression in a time dependent manner **[Fig. 2A-i].** Taken together, the results
367 demonstrated a significant reduction in promastigotes' growth and multiplication upon treatment with
368 **Gly 2**. Further we also assessed the potential role of anti-gp63 antibody against promastigote
369 proliferation. We found that there was subsequent change in percentage of CFDA positive cells in 24 h

370 (70.70%) compared to 48 h (50.27%) and 72 h (39.29%) respectively **[Fig. 2A-ii]**. It clearly indicated
371 that the raised polyclonal anti-Gp63 antibody could partially block promastigote proliferation for a short
372 period of time. Thus **Gly 2** proves to be effective enough in controlling promastigote proliferation as
373 compared to that of generated antibody.

374 **3.8 Anti-proliferative effect of Gly 2 led to destabilized redox potential in promastigotes.**

375 We investigated whether **Gly 2** mediated inhibition of LdGp63 disrupting multiplication could lead to
376 destabilization of the redox potential in promastigotes by measuring ROS levels using 2',7'–
377 dichlorofluorescin diacetate (DCFDA) [27] [28]. Within cells, ROS oxidizes DCFDA into 2',7'–
378 dichlorofluorescin (DCF) which is a green fluorogenic compound. Intense green fluorescence in Gly 2
379 treated promastigotes indicate enhanced intracellular ROS generation, in treated parasites. The
380 representative bar graph showed ~70% parasite population with DCFDA staining (DCFDA+/DCFDA-
381) indicative of elevated ROS levels **[Fig. 3A].**

382 **3.9 Gly2 interferes with mitochondrial function and disrupts mitochondrial membrane potential**
383 **(ΔΨm)**

384 Elevation of intracellular ROS coupled with the depolarization of mitochondria causing bioenergetics
385 catastrophe is the hallmark of cellular necrosis [27] [29]. The maintenance of mitochondrial ΔΨm is
386 vital for all metabolic processes and cell survival. To explore the effect of **Gly 2** on ΔΨm of
387 promastigotes, we have used a lipophilic, cationic dye (JC-1) exhibiting green fluorescence, which
388 enters the mitochondria and gets accumulated into a reversible complex known as J aggregates emitting
389 red fluorescence [30].The fluorescence intensity was evaluated using confocal microscopy. Enhanced
390 level of red fluorescence denotes more J aggregate formation due to higher ΔΨm, whereas shifting
391 towards lower red or accumulation of higher green fluorescence implies a strong indication of
392 destabilized ΔΨm. Notably, mitochondrial uptake of JC-1 dye was found to decrease with **Gly 2**
393 treatment as compared to control healthy promastigotes which is then manifested as stronger green
394 fluorescence due to monomeric JC-1 formation. Intense red fluorescence was observed in control
395 groups suggesting JC-1 aggregation due to stable ΔΨm **[Fig. 3B].**

396 **3.10 Gly 2 treated promastigotes enhances the complement mediated lysis in serum physiological**
397 **condition**

398 Mimicking the physiological condition of body, axenic promastigotes cultures in late log phase were
399 exposed to complement-mediated lysis, which was determined by measuring propidium iodide (PI)
400 stained cells [31] [32]. Histogram plots illustrate 50.02% population of promastigote death in 10%
401 Normal human serum (NHS) within 30 min as compared to control which showed 0.06 % parasite death
402 and 99.96% intact promastigotes in 10% FBS (heat inactivated). The **Gly 2** treated promastigotes
403 however showed 79.05% parasite death in the presence of 10% NHS. There was 29.48% increment in
404 PI uptake which is directly proportional to promastigote killing. Majority of **Gly 2** treated promastigotes
405 were non- motile when observed under the microscope. The precise size of this population is difficult
406 to calculate as, in the presence of NHS, promastigote cell volume and refractile properties are altered,
407 blurring the distinction between promastigotes, cell debris, and NHS background signal. These results
408 indicate that in the presence of **Gly 2** and 10% NHS causes rapid lysis Leishmania promastigote **[Fig.**
409 **4A].**

410 **3.11 Gly 2 inflicts cytotoxicity in Clinical PKDL strain BS12**

411 We further evaluated the effect the **Gly 2** on the clinical isolate of PKDL strain, BS12 of *L. donovani*
412 [33]. The results showed pronounced toxic effect of the **Gly 2** on the Indian origin leishmania isolate
413 of PKDL. As mentioned previously, LDH assay was carried out on promastigotes treated with different
414 concentrations of **Gly 2** for 72 h, while amphotericin B was used a positive control. The promastigotes
415 showed IC50 value at 1.93 µM with 50% parasitic death **[Fig. 4B].** Along with Gly 2, we also evaluated
416 the cytotoxic effects of 12 compounds on *L. donovani* promastigotes clinical isolate of PKDL strain at
417 5µM **(Supplementary Fig. 1B).** The data strongly suggests that **Gly2** could adversely affect the
418 metabolic cell viability of clinical strain of PKDL.

419 **2.12 *In-silico* docking of Gly 2 with 3D structure of *L. donovani*-Gp63 (LdGp63) protein identified**
420 **a druggable catalytic pocket bound to Gly 2.**

421 LdGp63 protein, a parasite receptor protein in its active form comprises of one chain containing multiple
422 beta sheets and helices, consisting of 590 residues. Using BLASTp, we found that LdGp63 showed
423 80.9% sequence identity with template (*L. major* leishmanolysin in complex Zinc ion, 1LML). We
424 performed homology modelling consequently with energy minimization for refined model of LdGp63
425 **[Fig. 5A & Supplementary Fig. 1E]**. Superimposition with this template rendered a RMSD value < 1
426 Å **[Fig. 5B].** Through RAMPAGE, we found that majority of residues were present in the favoured or
427 allowed regions of the Ramachandran plot, thus validating the quality of the homology model
428 **[Supplementary Fig. 1F]**. To evaluate the physical basis of protein-ligand interactions, we performed
429 *in-silico* docking studies of LdGp63 with all compounds **(Supplementary Fig.2A)**. The best
430 conformations of the docked compounds were selected based on their lowest free binding energy to the
431 catalytic domain. Analysis of this pocket unravelled three residues (**His251, Glu252** and **Pro334**) that
432 are involved in binding to the compounds **[Fig. 5C]. Gly 2** showed lower free binding energy as
433 compared to others suggesting efficient docking **[Table 3].** In the docked complex, the O3, O4 and O5
434 residue of Gly 2 formed a strong H-bond interaction with **His251, Glu252** and **Pro334** residues of
435 LdGP63 (2.83Å, 2.71 Å and 2.90 Å) respectively.

436 **3.13 Interaction of Gly 2 with LdGp63 enhances thermostability of protein-compound complex,**
437 **detected using cellular thermal shift assay (CETSA)**

438 Further to evaluate **Gly 2** dependent molecular mechanism involved in pathophysiological condition of
439 parasite leading to its death; we verified the binding efficacy of Gp63, potent virulence factor with **Gly**
440 **2** inhibitor in promastigote lysates using cellular thermal shift assay **(CETSA)** [34]. The recently
441 developed CETSA showed that target engagement can likewise be assessed in whole cell lysates based
442 on altered protein thermostability [35], thus allows the investigation of target assignation under
443 pathological conditions. We first titrated the number of promastigotes (10^4-10^7 cells) and
444 immunoblotted with anti-Gp63 antibody **[Fig. 5D].** We then focused on treated and untreated
445 promastigote lysates (10^7 cells), which were incubated with **Gly 2** (5µM) or vehicle for 24 h and
446 subsequently exposed to different temperatures before immunoblotting. The results of the immunoblot
447 showed that the abundance of Gp63 Catalytic domain in the cell lysate decreased with increasing

448 temperatures (4−80 °C). Importantly, in the range from 60 to 80 °C, the lysates treated with **Gly 2**
449 showed abundances of Catalytic Domain of Gp63 protein higher than the abundances of the same
450 protein in untreated**.** There was a drastic reduction in area intensity of bands in the promastigotes lysate
451 at the temperature of 80°C which was measured to be 1842.062 as compared to Gly 2 treated
452 promastigotes lysate which was indicated to be 20749.413 at similar conditions. The control lanes of
453 4°C constituting both untreated and Gly 2 treated parasite lysates exhibited area intensity of 20812.383
454 and 20755.839, respectively. This clearly suggested ligand-dependent stabilization by Gly 2 even at
455 much higher temperature than the normal physiological temperature **[Fig. 5E].**

456 **4. DISCUSSION**

457 The major blockades towards effective treatment against leishmaniasis include pharmacokinetics and
458 pharmacodynamics of drugs, toxicity, expensive, drug resistance, lack of vaccines and inadequate
459 therapeutic interventions Successful treatment of cutaneous leishmaniasis with amphotericin B; a case
460 of unresponsive to pentavalent antimony therapy [7]. The major prevention strategy involves protection
461 of host from the bite of sand fly, which is an infeasible task. This creates a new pavement for discovering
462 novel drug targets and developing target specific molecules; for better preventive measures and
463 treatment modalities [36]. Recent unexplored area in the field of therapeutics against VL mainly
464 focusses on transmission blocking drugs. Thus, targeting specific enzymes which are involved in
465 cellular metabolism of promastigotes with transmission blocking drugs is an effective alternative
466 strategy for efficient therapeutic implications [37].

467 Gp63/ Leishmanolysin belongs to a family of metalloproteinase which share the common signature
468 sequence of HE*XX*H as a conserved zinc-binding/catalytic motif [38] [39]. It is present extracellularly
469 on promastigote surface found in gut of the insect vector and intralysosomally parasitize macrophages
470 as amastigotes in the mammalian host, causing human leishmaniasis. Gp63 has been suggested to
471 function in multiple steps of the infection [40], i.e. their entry into macrophages [41] and intralysosomal
472 survival [19] [42]. Gp63/Leishmanolysin thus appears to differ functionally from other HEXXH
473 metalloproteinase families. Earlier reports elucidated the potent role of flavonoid glycosides from
474 biologically active aqueous plant extracts against VL [43].

475 Based on these facts we have synthesized simple glucose and glucosamine backbone conferring natural
476 product inspired library of Gp63 inhibitors using green chemistry approach. Upon screening of
477 glycoside derivatives on *L. donovani* promastigotes, we found that **Gly 2, 6** and **8** imposed profound
478 cytotoxic effects with no lethal effect in mammalian cells such as macrophages and canine epithelial
479 cells, MDCK ensuring their specificity towards *L. donovani* promastigotes but not on host. The
480 specificity was further assessed by their selectivity index ratio (CC50 for host cells/IC50 for parasite).
481 The lead glycosides were more selective for *L. donovani* parasites than the host cells, with a selectivity
482 index ratio of >1000. The low toxicity against mammalian cells is an important criterion while exploring
483 new active compounds with anti-parasitic activity. The chemical structure of compounds is yet another
484 essential factor related to their role as antileishmanials. The most active compound **Gly 2** derived from
485 D-glucose have isopentyl as branched alkyl group with native free OH group which make the molecule
486 hydrophilic (clogP 0.26) and less penetrable into cell. Whereas other active compound **Gly 6** having
487 isopentyl as branched alkyl chain and hydroxyl group were masked with acetyl (OAc) group thus
488 making molecule more hydrobhobic (clogP 2.4) suitable for cell permeability. The designed inhibitors
489 were in fact supported by our *in-silico* experimental results where **Gly 2** is binding on the surface of the
490 parasite (*Leishmania* promastigotes) whereas **Gly 6** easily penetrable through the cell surface. **Gly 8**
491 were having shorter straight or linear alkyl chain (propyl) along with masked hydroxyl group making
492 its amphiphilic (clogP 1.47) molecule that can perform dual role which includes surface binding
493 probability and penetration inside the cell. We further validated the toxic effect of lead glycoside
494 derivatives on promastigotes with Hoechst and PI staining leading to parasite death. We found that **Gly**
495 **2, 6** and **8** showed more PI+ and less Hoechst+ cells as compared to control promastigotes which
496 depicted visa-versa. **Gly 2** showed highest PI+ among other two lead glycosides without induction of
497 phospholipids exposure on the plasma membrane (data not provided).

498 To understand the cellular consequences of *in-vitro* inhibition of **Gly 2** promastigotes, we have
499 investigated the promastigote proliferation. Using live staining with CFDA-SE (a strong membrane
500 permeant dye), the effect of **Gly 2** treatment on promastigotes the growth kinetics of promastigotes was
501 studied. The CFDA-SE dye upon cleavage by esterases within the cell, generates reactive amine

502 products that covalently bonds with intracellular lysine to generate fluorescence. Based on this assay,
503 the **Gly 2** treated promastigotes showed complete abrogation of cell division / progression at
504 consecutive days. We even masked the promastigote surface with generated mouse polyclonal anti-
505 LdGp63 catalytic domain antibody at a dilution of 1:400; interestingly found that such treatment lead
506 to partial abrogation of promastigote proliferation.

507 Based on our proposition, **Gly 2** treatment lead to repudiation of promastigotes further causing
508 increased ROS generation whereas control parasites showed balanced redox homeostasis. Further, it
509 has been reported that drug-induced loss in ΔΨm is associated with cellular death in *L. donovani, L.*
510 *amazonensis and Trypanosoma cruzi* [44]. ΔΨm loss and ROS elevation are coupled events and act as
511 crucial signals of necrosis [45]. Thus, we then determined ΔΨm loss following increased load of
512 oxidative stress in **Gly 2** treated promastigotes leading to necrosis like death which was corroborated
513 with PI positivity proved earlier.

514 Later mimicking pathophysiological conditions of the body, we tried to elucidate the susceptibility of
515 promastigotes towards complement mediated lysis. We propagated promastigotes in the presence of
516 10% NHS and after 15 min of incubation, 50% cellular death in control promastigotes was observed
517 through incorporation of PI. In contrast to control parasites, there was 29% increment of parasite death
518 in **Gly 2** treated samples, depicting 79% cytolysis.

519 Encouraged by these results, we evaluated the efficacy of **Gly 2** on clinical PKDL isolate BS12, which
520 is responsible for the post kalazar disease manifestation, and known to play crucial role for *L. donovani*
521 during interepidemic periods. It was observed that **Gly 2** leads to significant growth inhibition in BS12
522 at much lower concentration of 1.97μM>= IC50.
523 After confirmation of cytotoxic and downstream cellular effects on promastigotes of lab and clinical
524 strains, we adopted an *in-silico* and *in-vitro* based Gp63 inhibition study. This was in accordance with
525 previous reports suggesting role of Gp63 in promastigote multiplication [46]. The fundamental aim of
526 the study was to ensure enhanced efficacy of the lead compound based on structure-to-activity
527 relationships. Sequence and structure alignment between LmGp63 and LdGp63 show conserved
528 Histidine triad as catalytic residues (His251, His254 and His320) in LDGp63. The *in-silico* docking

529 study suggested that **Gly 2** is efficiently docking to Gp63 with low free binding energy, whereas docking
530 with other compounds was inefficient. The **Gly 2** binding pocket represents an optimal volume (82 X
531 74 X 75 $Å^3$) around catalytic domain for efficient binding to catalytic residues in the protein. Out of 12
532 molecules three of them (Gly 1, Gly 2, Gly 3) showed lower minimum binding energies such as -4.61,
533 -8.4, -5.38 Kcal/mol respectively. However minimum binding energy of **Gly 2** is lowest as well as it
534 interacts with the His251 residue present in the active site pocket of GP63. Among 12 glycosides, **Gly**
535 **2** shows strong hydrogen bond interaction with His251, Glu252 and Pro334. **Gly 2** also forms
536 hydrophobic interactions around residues of LdGp63 catalytic pocket that assist it to fit in the catalytic
537 pocket.

538 Further to assess strong interactions between a drug and its protein target in a physiologically relevant
539 cellular environment we performed CETSA. Previous studies showed that CETSA has been performed
540 in complex protein samples and in live cells displaying an altered melting or aggregation behaviour
541 upon exposure to increased temperature [47]. CETSA has also been employed to identify *Plasmodium*
542 *falciparum* protein targets in parasite lysates [48]. In this study, we have used target-specific antibodies
543 that is antibody against catalytic domain Gp63. We found that on binding of **Gly 2** with Gp63; caused
544 protein stabilization event under physiologic conditions even at remarkably high temperature of 60-
545 80°C. Normally, at higher temperature protein denaturation takes place. But when the ligand is binding
546 strongly to binding pocket of the protein; it affects both conformation and stability of the protein of
547 interest. This was prominently observed when we immunoblotted the membrane with anti-LdGp63
548 catalytic domain antibody and found abundances of Catalytic Domain of Gp63 protein in treated
549 samples. This suggested that there might be possibility that **Gly 2** has higher affinity in binding towards
550 catalytic domain of Gp63.

551 Previously, there were reports suggesting that apoptotic parasites contribute towards macrophage
552 invasion by balancing the ratio of viable to non-viable parasites as 1:1. However, our results
553 demonstrated that more than 90% of **Gly 2** treated parasites are undergoing cellular death. Therefore,
554 we hypothesize that the treatment with the **Gly 2** molecule will significantly reduce the number of
555 parasites available for infection in macrophages. The results demonstrated potential effect on

556 intracellular amastigotes at nanomolar range suggesting their strong anti-leishmanial activity in
557 macrophage infection model. Details of the strategy have been explained in the working model.

558 **5. CONCLUSIONS**

559 In current scenario there is an estimation of 0·7–1 million newly reported cases of leishmaniasis
560 erupting out every year from the 100 endemic countries globally. Thus, there is a requirement to develop
561 new potent antileishmanial which are less prone to resistance development. Conclusively, we have
562 introduced a novel glycoside derivative, Gly 2 as potential anti-leishmanial and suggested a prospective
563 first in class therapeutic measure for both Kala azar and post kala azar dermal (PKDL) leishmaniasis
564 respectively to ascertain their clinical utility.

565 **Conflicts of interest**

566 The authors declare that they have no conflicts of interest with the contents of this article.

567 **Funding**

568 This work was supported by funding from DBT builder program, DST, and JNU UPE II program. Dr.
569 Shailja Singh is thankful for the funding support from Science and Engineering Research Board (SERB,
570 File no. IPA/2020/000007) and Drug and Pharmaceuticals Research Programe (DPRP, Project No.
571 P/569/2016-1/TDT. Dr. Soumya Pati is greatful for the funding support from Cognitive Science
572 Research Initiative (CSRI) program of Department of Science and Technology (DST/CSRI/2018/247).

573 **Acknowledgements**

574 AC and NJ are supported by Shiv Nadar Foundation fellowships. Center for Informatics located within
575 Shiv Nadar University is also duly acknowledged. SG is thankful for the funding support from DST
576 INSPIRE grant. SP is grateful for the funding support from Shiv Nadar foundation. CN acknowledges
577 the fellowship supported by CSIR-NET. We sincerely acknowledge help from Prof. Madhubala
578 Rentala, JNU for gifting the J774.A1 murine macrophage cell line.

579

580 **References**

581 [1] R. Arenas, E. Torres-Guerrero, M.R. Quintanilla-Cedillo, J. Ruiz-Esmenjaud, Leishmaniasis:
582 A review, F1000Research. (2017). https://doi.org/10.12688/f1000research.11120.1.

583 [2] E.E. Zijlstra, The immunology of post-kala-azar dermal leishmaniasis (PKDL), Parasites and
584 Vectors. (2016). https://doi.org/10.1186/s13071-016-1721-0.

585 [3] P. Desjeux, Leishmaniasis: Current situation and new perspectives, Comp. Immunol.
586 Microbiol. Infect. Dis. (2004). https://doi.org/10.1016/j.cimid.2004.03.004.

587 [4] S. Burza, S.L. Croft, M. Boelaert, Leishmaniasis, Lancet. (2018).
588 https://doi.org/10.1016/S0140-6736(18)31204-2.

589 [5] S.L. Croft, S. Sundar, A.H. Fairlamb, Drug resistance in leishmaniasis, Clin. Microbiol. Rev.
590 (2006). https://doi.org/10.1128/CMR.19.1.111-126.2006.

591 [6] A. Ponte-Sucre, F. Gamarro, J.C. Dujardin, M.P. Barrett, R. López-Vélez, R. García-
592 Hernández, A.W. Pountain, R. Mwenechanya, B. Papadopoulou, Drug resistance and
593 treatment failure in leishmaniasis: A 21st century challenge, PLoS Negl. Trop. Dis. (2017).
594 https://doi.org/10.1371/journal.pntd.0006052.

595 [7] Y. Yeşilova, E. Turan, H.A. ltı. Sürücü, M. Aksoy, A. Özbilgin, Successful treatment of
596 cutaneous leishmaniasis with amphotericin B; a case of unresponsive to pentavalent antimony
597 therapy, Turkiye Parazitol. Derg. (2015). https://doi.org/10.5152/tpd.2015.3761.

598 [8] R. Sen, M. Chatterjee, Plant derived therapeutics for the treatment of Leishmaniasis,
599 Phytomedicine. (2011). https://doi.org/10.1016/j.phymed.2011.03.004.

600 [9] O.P. Singh, B. Singh, J. Chakravarty, S. Sundar, Current challenges in treatment options for
601 visceral leishmaniasis in India: A public health perspective, Infect. Dis. Poverty. (2016).
602 https://doi.org/10.1186/s40249-016-0112-2.

603 [10] J. Sunter, K. Gull, Shape, form, function and Leishmania pathogenicity: from textbook
604 descriptions to biological understanding, Open Biol. (2017).
605 https://doi.org/10.1098/rsob.170165.

606 [11] C. Yao, J.E. Donelson, M.E. Wilson, The major surface protease (MSP or GP63) of
607 Leishmania sp. Biosynthesis, regulation of expression, and function, Mol. Biochem. Parasitol.
608 (2003). https://doi.org/10.1016/S0166-6851(03)00211-1.

609 [12] R.J. Etges, J. Bouvier, R. Hoffman, C. Bordier, Evidence that the major surface proteins of
610 three Leishmania species are structurally related, Mol. Biochem. Parasitol. (1985).
611 https://doi.org/10.1016/0166-6851(85)90033-7.

612 [13] S. Kamhawi, Phlebotomine sand flies and Leishmania parasites: friends or foes?, Trends
613 Parasitol. (2006). https://doi.org/10.1016/j.pt.2006.06.012.

614 [14] G. Chaudhuri, K.P. Chang, Acid protease activity of a major surface membrane glycoprotein
615 (gp63) from Leishmania mexicana promastigotes, Mol. Biochem. Parasitol. (1988).
616 https://doi.org/10.1016/0166-6851(88)90023-0.

617 [15] C. Yao, K.G. Leidal, A. Brittingham, D.E. Tarr, J.E. Donelson, M.E. Wilson, Biosynthesis of
618 the major surface protease GP63 of Leishmania chagasi, Mol. Biochem. Parasitol. (2002).
619 https://doi.org/10.1016/S0166-6851(02)00030-0.

620 [16] B.S. McGwire, K.P. Chang, D.M. Engman, Migration through the extracellular matrix by the
621 parasitic protozoan Leishmania is enhanced by surface metalloprotease gp63, Infect. Immun.
622 (2003). https://doi.org/10.1128/IAI.71.2.1008-1010.2003.

623 [17] P.B. Joshi, D.L. Sacks, G. Modi, W.R. McMaster, Targeted gene deletion of Leishmania major
624 genes encoding developmental stage-specific leishmanolysin (GP63), Mol. Microbiol. (1998).
625 https://doi.org/10.1046/j.1365-2958.1998.00689.x.

626 [18] P.B. Joshi, B.L. Kelly, S. Kamhawi, D.L. Sacks, W.R. McMaster, Targeted gene deletion in
627 Leishmania major identifies leishmanolysin (GP63) as a virulence factor, Mol. Biochem.
628 Parasitol. (2002). https://doi.org/10.1016/S0166-6851(01)00432-7.

629 [19] A. Brittingham, C.J. Morrison, W.R. McMaster, B.S. McGwire, K.-P. Chang, D.M. Mosser,
630 Role of the Leishmania surface protease gp63 in complement fixation, cell adhesion, and
631 resistance to complement-mediated lysis, Parasitol. Today. (1995).

632 https://doi.org/10.1016/0169-4758(95)80054-9.

633 [20] P.J. Dunn, A.S. Wells, M.T. Williams, Green Chemistry in the Pharmaceutical Industry, 2010.
634 https://doi.org/10.1002/9783527629688.

635 [21] I. Prassas, E.P. Diamandis, Novel therapeutic applications of cardiac glycosides, Nat. Rev.
636 Drug Discov. (2008). https://doi.org/10.1038/nrd2682.

637 [22] N. Goyal, S. Cheuk, G. Wang, Synthesis and characterization of d-glucosamine-derived low
638 molecular weight gelators, Tetrahedron. (2010). https://doi.org/10.1016/j.tet.2010.05.071.

639 [23] A. Daina, O. Michielin, V. Zoete, SwissADME: A free web tool to evaluate pharmacokinetics,
640 drug-likeness and medicinal chemistry friendliness of small molecules, Sci. Rep. (2017).
641 https://doi.org/10.1038/srep42717.

642 [24] H. Kaushik, S. Deshmukh, D.D. Mathur, A. Tiwari, L. C. Garg, Recombinant expression of in
643 silico identified B-cell epitope of epsilon toxin of Clostridium perfringens in translational
644 fusion with a carrier protein, Bioinformation. (2013).
645 https://doi.org/10.6026/97320630009617.

646 [25] M.J. Waring, Lipophilicity in drug discovery, Expert Opin. Drug Discov. 5 (2010) 235–248.
647 https://doi.org/10.1517/17460441003605098.

648 [26] I. Messaritakis, A. Mazeris, E. Koutala, M. Antoniou, Leishmania donovani s.l.: Evaluation of
649 the proliferation potential of promastigotes using CFSE staining and flow cytometry, Exp.
650 Parasitol. (2010). https://doi.org/10.1016/j.exppara.2010.03.006.

651 [27] M.J. Corral, E. Benito-Peña, M.D. Jiménez-Antón, L. Cuevas, M.C. Moreno-Bondi, J.M.
652 Alunda, Allicin Induces Calcium and Mitochondrial Dysregulation Causing Necrotic Death in
653 Leishmania, PLoS Negl. Trop. Dis. (2016). https://doi.org/10.1371/journal.pntd.0004525.

654 [28] D. Ramu, S. Garg, R. Ayana, A.K. Keerthana, V. Sharma, C.P. Saini, S. Sen, S. Pati, S. Singh,
655 Novel β-carboline-quinazolinone hybrids disrupt Leishmania donovani redox homeostasis and
656 show promising antileishmanial activity, 2017. https://doi.org/10.1016/j.bcp.2016.12.012.

657 [29] W.X. Zong, C.B. Thompson, Necrotic death as a cell fate, Genes Dev. (2006).
658 https://doi.org/10.1101/gad.1376506.

659 [30] F. Sivandzade, A. Bhalerao, L. Cucullo, Analysis of the Mitochondrial Membrane Potential
660 Using the Cationic JC-1 Dye as a Sensitive Fluorescent Probe, BIO-PROTOCOL. 9 (2019).
661 https://doi.org/10.21769/BioProtoc.3128.

662 [31] S. Bandyopadhyay, M. Chatterjee, T. Das, S. Bandyopadhyay, S. Sundar, C. Mandal,
663 Antibodies Directed against O -Acetylated Sialoglycoconjugates Accelerate Complement
664 Activation in Leishmania donovani Promastigotes , J. Infect. Dis. (2004).
665 https://doi.org/10.1086/425519.

666 [32] M. Domínguez, I. Moreno, M. López-Trascasa, A. Toraño, Complement interaction with
667 trypanosomatid promastigotes in normal human serum, J. Exp. Med. (2002).
668 https://doi.org/10.1084/jem.20011319.

669 [33] R. Sengupta, S.J. Chowdhury, S. Moulik, M.K. Ghosh, B. Saha, N.K. Das, M. Chatterjee,
670 Active surveillance identified a neglected burden of macular cases of Post Kala-azar Dermal
671 Leishmaniasis in West Bengal, PLoS Negl. Trop. Dis. (2019).
672 https://doi.org/10.1371/journal.pntd.0007249.

673 [34] H. Almqvist, H. Axelsson, R. Jafari, C. Dan, A. Mateus, M. Haraldsson, A. Larsson, D.M.
674 Molina, P. Artursson, T. Lundbäck, P. Nordlund, CETSA screening identifies known and
675 novel thymidylate synthase inhibitors and slow intracellular activation of 5-fluorouracil, Nat.
676 Commun. (2016). https://doi.org/10.1038/ncomms11040.

677 [35] H. Axelsson, H. Almqvist, B. Seashore-Ludlow, T. Lundbäck, Screening for Target
678 Engagement using the Cellular Thermal Shift Assay - CETSA, 2004.

679 [36] F. Chappuis, S. Sundar, A. Hailu, H. Ghalib, S. Rijal, R.W. Peeling, J. Alvar, M. Boelaert,
680 Visceral leishmaniasis: What are the needs for diagnosis, treatment and control?, Nat. Rev.
681 Microbiol. (2007). https://doi.org/10.1038/nrmicro1748.

682 [37] K. Jain, N.K. Jain, Vaccines for visceral leishmaniasis: A review, J. Immunol. Methods.

683 (2015). https://doi.org/10.1016/j.jim.2015.03.017.

684 [38] N. Cerdà-Costa, F.X. Gomis-Rüth, Architecture and function of metallopeptidase catalytic
685 domains, Protein Sci. (2014). https://doi.org/10.1002/pro.2400.

686 [39] B.S. McGwire, K.-P. Chang, Posttranslational Regulation of a Leishmania HE XX H
687 Metalloprotease (gp63) , J. Biol. Chem. (1996). https://doi.org/10.1074/jbc.271.14.7903.

688 [40] A. Brittingham, G. Chen, B.S. Mcgwire, K.P. Chang, D.M. Mosser, Interaction of Leishmania
689 gp63 with cellular receptors for fibronectin, Infect. Immun. (1999).
690 https://doi.org/10.1128/iai.67.9.4477-4484.1999.

691 [41] X. Liu, K.P. Chang, Extrachromosomal genetic complementation of surface metalloproteinase
692 (gp63)-deficient Leishmania increases their binding to macrophages, Proc. Natl. Acad. Sci. U.
693 S. A. (1992). https://doi.org/10.1073/pnas.89.11.4991.

694 [42] K.P. Soteriadou, M.S. Remoundos, M.C. Katsikas, A.K. Tzinia, V. Tsikaris, C. Sakarellos, S.J.
695 Tzartos, The Ser-Arg-Tyr-Asp region of the major surface glycoprotein of Leishmania mimics
696 the Arg-Gly-Asp-Ser cell attachment region of fibronectin, J. Biol. Chem. (1992).

697 [43] N.A. Shah, M.R. Khan, A. Nadhman, Antileishmanial, toxicity, and phytochemical evaluation
698 of medicinal plants collected from Pakistan, Biomed Res. Int. (2014).
699 https://doi.org/10.1155/2014/384204.

700 [44] R. Andréo, L.O. Regasini, M.S. Petrônio, B.G. Chiari-Andréo, A. Tansini, D.H.S. Silva,
701 R.M.B. Cicarelli, Toxicity and Loss of Mitochondrial Membrane Potential Induced by Alkyl
702 Gallates in Trypanosoma cruzi , Int. Sch. Res. Not. (2015).
703 https://doi.org/10.1155/2015/924670.

704 [45] N. Festjens, T. Vanden Berghe, P. Vandenabeele, Necrosis, a well-orchestrated form of cell
705 demise: Signalling cascades, important mediators and concomitant immune response,
706 Biochim. Biophys. Acta - Bioenerg. (2006). https://doi.org/10.1016/j.bbabio.2006.06.014.

707 [46] S. Pandey, P. Chakraborti, R. Sharma, S. Bandyopadhyay, D. Sarkar, S. Adhya, Involvement

of Leishmania donovani major surface glycoprotein gp63 in promastigote multiplication, J. Biosci. (2004). https://doi.org/10.1007/BF02702557.

[47] A. Langebäck, S. Bacanu, H. Laursen, L. Mout, T. Seki, S. Erkens-Schulze, A.D. Ramos, A. Berggren, Y. Cao, J. Hartman, W. van Weerden, J. Bergh, P. Nordlund, S. Lööf, CETSA-based target engagement of taxanes as biomarkers for efficacy and resistance, Sci. Rep. (2019). https://doi.org/10.1038/s41598-019-55526-8.

[48] J.M. Dziekan, H. Yu, D. Chen, L. Dai, G. Wirjanata, A. Larsson, N. Prabhu, R.M. Sobota, Z. Bozdech, P. Nordlund, Identifying purine nucleoside phosphorylase as the target of quinine using cellular thermal shift assay, Sci. Transl. Med. (2019). https://doi.org/10.1126/scitranslmed.aau3174.

Table 1: The structures of all the glycosides (1-12) are depicted.

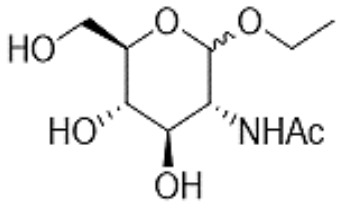 **Gly 1**	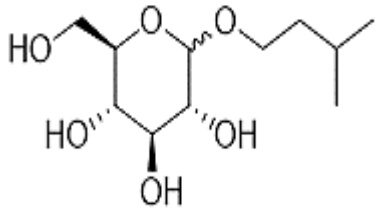 **Gly 2**	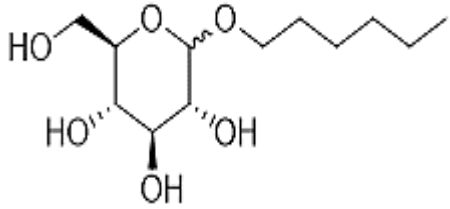 **Gly 3**
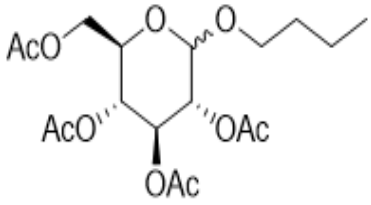 **Gly 4**	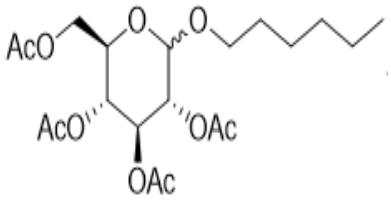 **Gly 5**	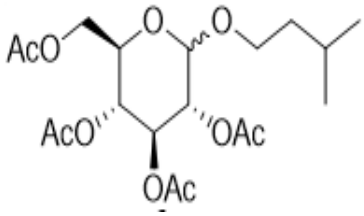 **Gly 6**
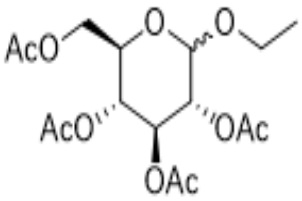 **Gly 7**	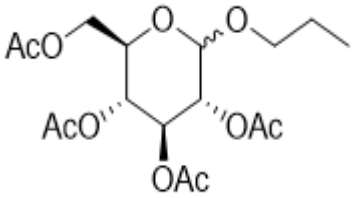 **Gly 8**	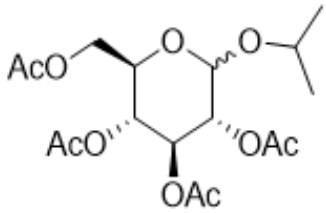 **Gly 9**
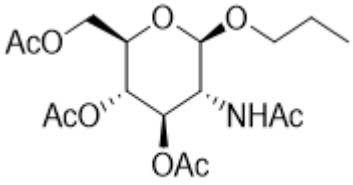 **Gly 10**	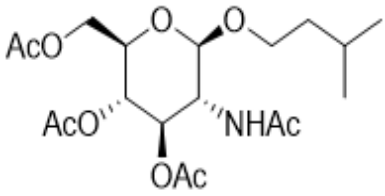 **Gly 11**	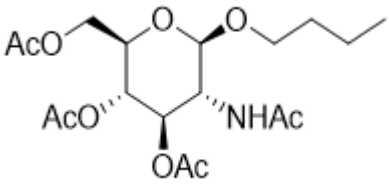 **Gly 12**

763

764 **Table 2: IC50/CC50/SI values of Gly 2**

	IC_{50} (µM)	CC_{50} (µM) MDCK	SI MDCK	CC_{50} (µM) Macrophages	SI Macrophages
Gly 2	1.13	2100	1858.407	2900	2566.371
Gly 1	65	298	4.584	247.9	3.813
Gly 3	12.7	1890	148.818	1677.6	132.090
Gly 4	4.6	159	34.565	167	36.304
Gly 5	5.97	177	29.648	159.2	26.666
Gly 6	3.4	1070	314.705	1033	303.823
Gly 7	77	297	3.857	299	3.883
Gly 8	1.6	818	511.25	959	599.375
Gly 9	36	187	5.194	256	7.111
Gly 10	25.22	176	6.978	239	9.476
Gly 11	43	165	3.837	179	4.162
Gly 12	95	287	3.021	279	2.936

765

766

767

768

769

770

Table 3: Critical residues lying within the docked ligand-protein complex were found to be forming H-bonds with highest minimum binding energy with Gly 2.

Compounds	Structure	Minimum binding energy	No. of H- bonds involved
Gly 1	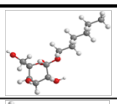	-4.61	3
Gly 2	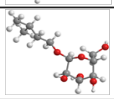	-8.4	3
Gly 3	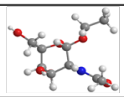	-5.38	2
Gly 4	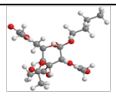	-3.92	2
Gly 5	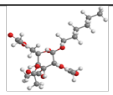	-3.35	1
Gly 6	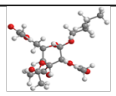	-5.42	2
Gly 7	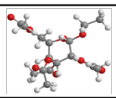	-4.82	2
Gly 8	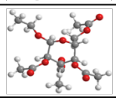	-4.89	2
Gly 9	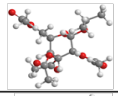	-2.87	3
Gly 10	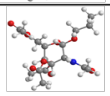	-4.85	2
Gly 11	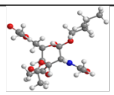	-3.76	2
Gly 12	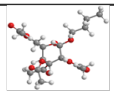	-4.35	1

Figure legends:

[**Figure 1:** Scheme of synthesis of glycoside derivatives and concentration dependent effect of potent novel glycosides on promastigotes of Ag83 strain with variable membrane binding affinity. (A) Synthesis of designed glycosides was carried out with commercially available D-glucose and D-glucosamine coupling with various short to long chain alcohols under acidic condition; (B) Percentage

781 inhibition of promastigotes treated with Gly 2 was evaluated using LDH Assay for 72 h and plotted as
782 sigmoidal curve. Data normalization was done by taking into consideration the cytotoxicity induced by
783 positive control (amphotericin B-3 µg/ml) as 100%. IC50 values for promastigotes of Ag83 strain were
784 analysed using GraphPad Prism, represented as the mean ± SD where n=3, independent experiments;
785 (C-i) the representative screenshots of PI stained promastigotes at 72 h assessed by fluorescence
786 microscopy depicting parasite death on glycoside treatment; (C-ii) percentage Propidium Iodide (PI)
787 positivity of the promastigotes at 72 h when treated by novel glycoside; (D) Membrane binding affinity
788 of Glycosides 2,6 and 8 using PerMM server.]

789 [**Figure 2:** Effect of Gly 2 on promastigote proliferation using flow cytometry. Nominal decrement
790 observed in percentage of CFDA-SE positive promastigotes when treated by compound for 24 h, 48 h
791 and 72 h. The asterisks (**) indicate statistical significance ($p < 0.01$, n=3) between the indicated
792 groups.]

793 [**Figure 3:** Gly 2 efficiently reduce promastigote proliferation activity leading to elevated ROS levels
794 and disrupting mitochondrial membrane potential of glycoside treated promastigotes. A) Confocal
795 imaging of DCFDA staining showed strong green fluorescence in Gly 2 treated cells, indicative of
796 increased ROS levels. Presence of green fluorescence in treated parasites was observed in treated
797 control, B) Effect of Gly 2 on ΔΨm of Ag83 promastigotes indicated by the conversion in monomer to
798 oligomer forms of JC-1 using confocal micrographs. The shift in intensity of red fluorescence (JC1
799 aggregates/PE) to green fluorescence (JC1 monomers/FITC) implies ΔΨm in promastigotes following
800 the treatment.]

801 [**Figure 4: Gly 2** treated promastigotes enhances the complement mediated lysis in serum physiological
802 condition and its concentration dependent cytotoxic effect on PKDL strain. A) Promastigote lysis was
803 analysed by uptake of PI using flowcytometry triggered by 10% Normal human serum; B) Cytotoxic
804 effect of **Gly 2** on clinical PKDL isolate BS12 in concentration dependent manner.]

805 [**Figure 5:** *In-silico* docking of Glycoside 2 **(Gly 2)** with 3D structure of *L. donovani*-Gp63 (LdGp63)
806 protein and *In-vitro* binding assay for potent LdGp63 inhibitor **(Gly 2)** in promastigote cell lysates using

807 CETSA. A) RMSD value of LdGp63 model showed significant changes in stability post energy
808 minimization; B) Superimposition of LdGp63 and LmGp63 models showed significant structure
809 identity; C) 3D surface model of Gly 2-LdGp63 complex denoted by degree of hydrophobicity and
810 surface accessible for ligand binding using a grey scheme. The defined region shows interacting
811 residues of Gly 2-LdGp63 complex; D) LdGp63 was detected in variable number of promastigote lysate
812 with generated polyclonal anti-LdGp63 antibody; cropped blots has been displayed, the full-length
813 blots are included in a Supplementary Information figure; E) the thermostability of LdGp63 was
814 analysed by immunoblotting following heat treatment at a range from 4 °C to 80 °C temperatures in
815 treated or untreated promastigotes with Gly 2 (5µM) depicted as cropped blots from different gels.]

816 [**Figure-6 :**Working model for discovery and translational application of **Gly 2.**]

817

818

819

Figure. 1

A

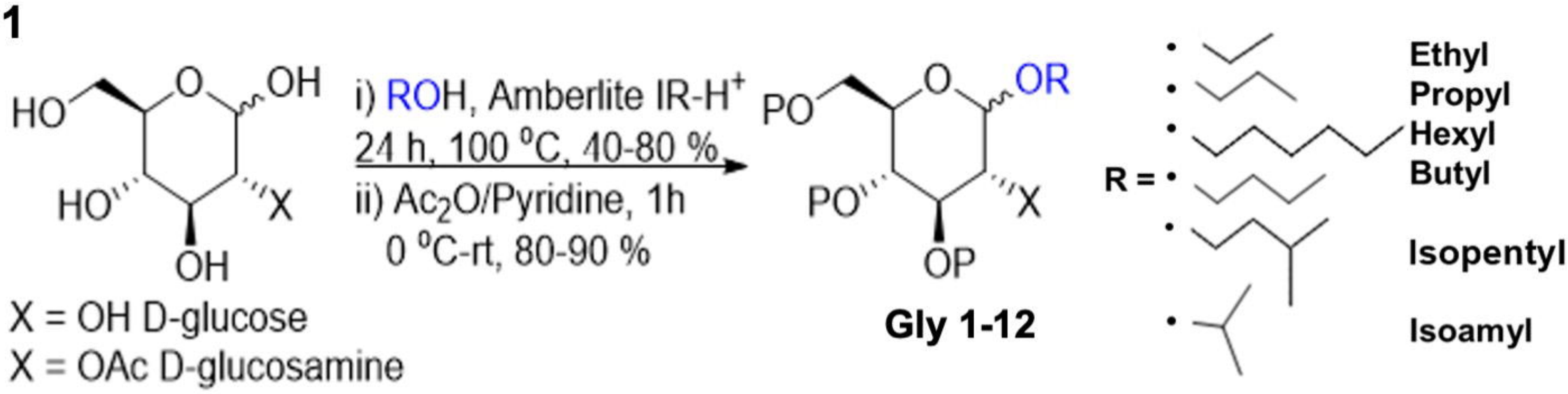

B

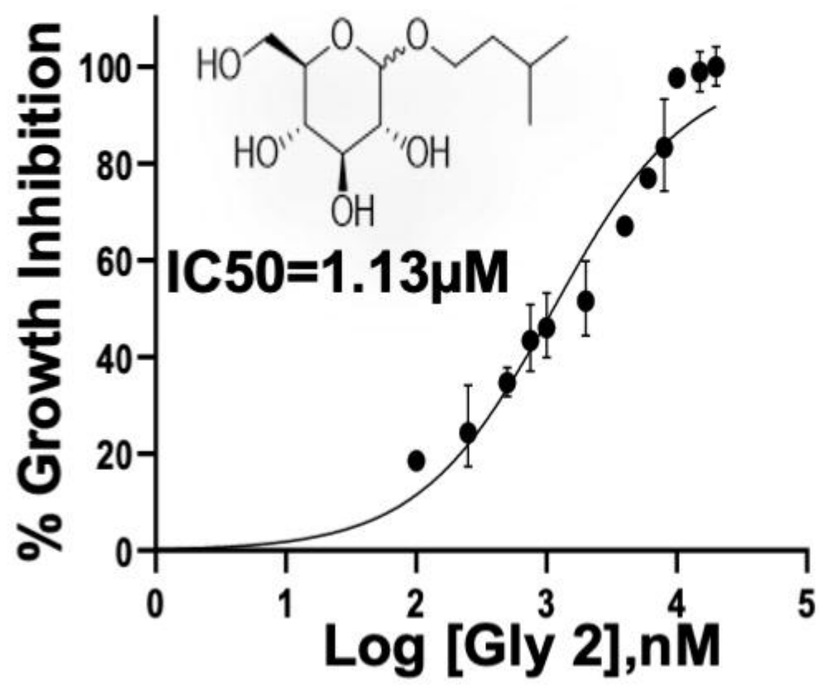

C

i)

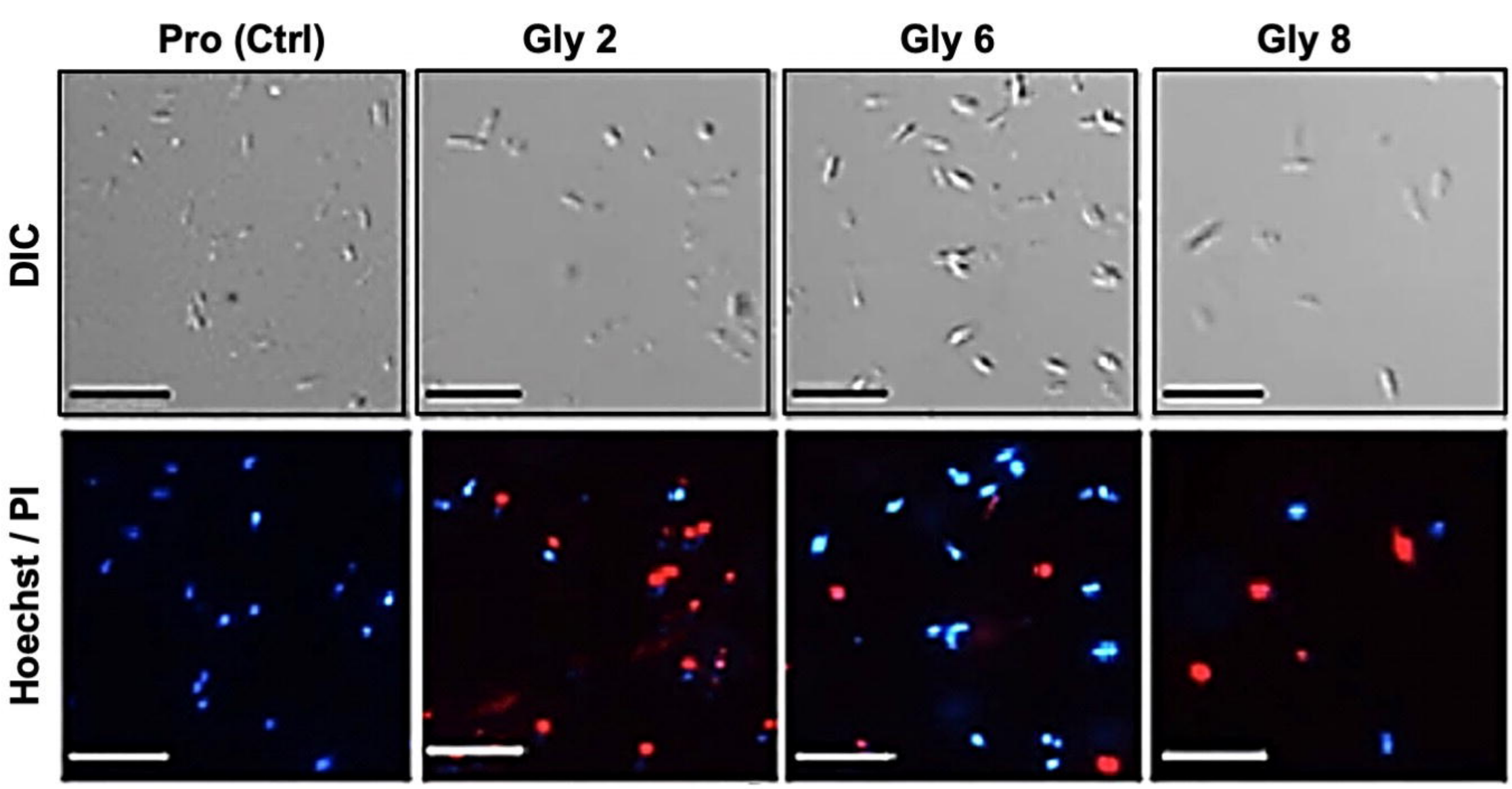

D

ii)

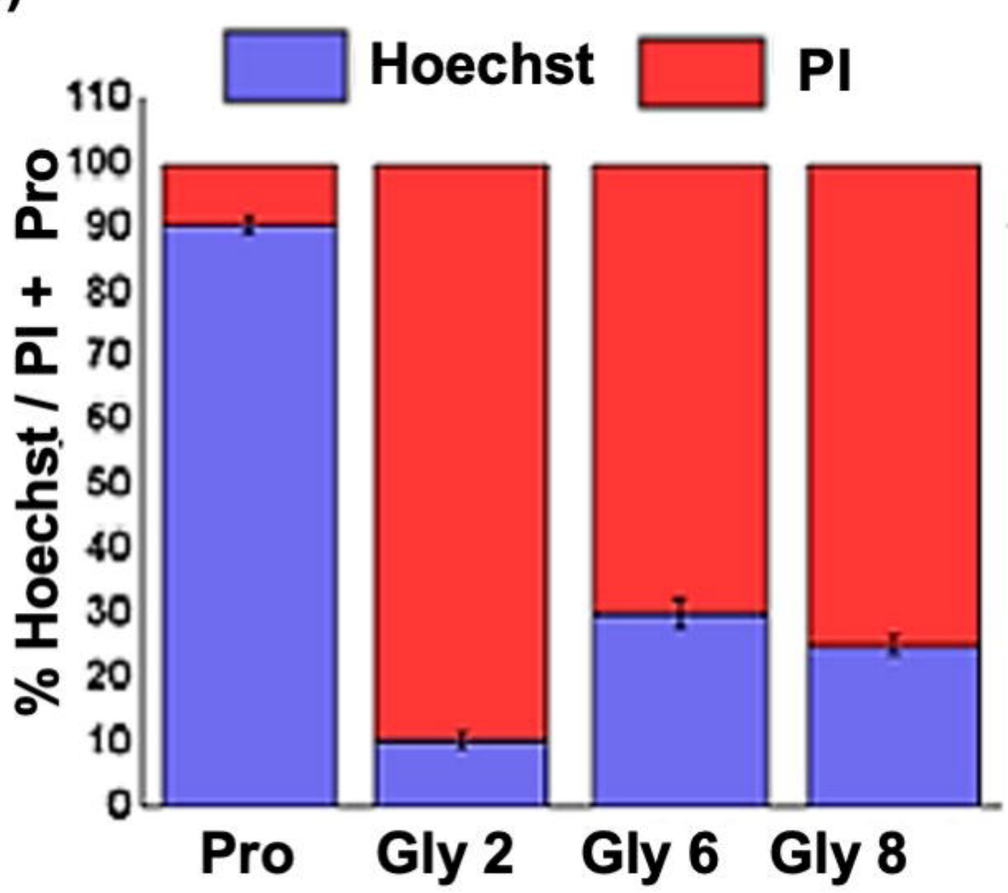

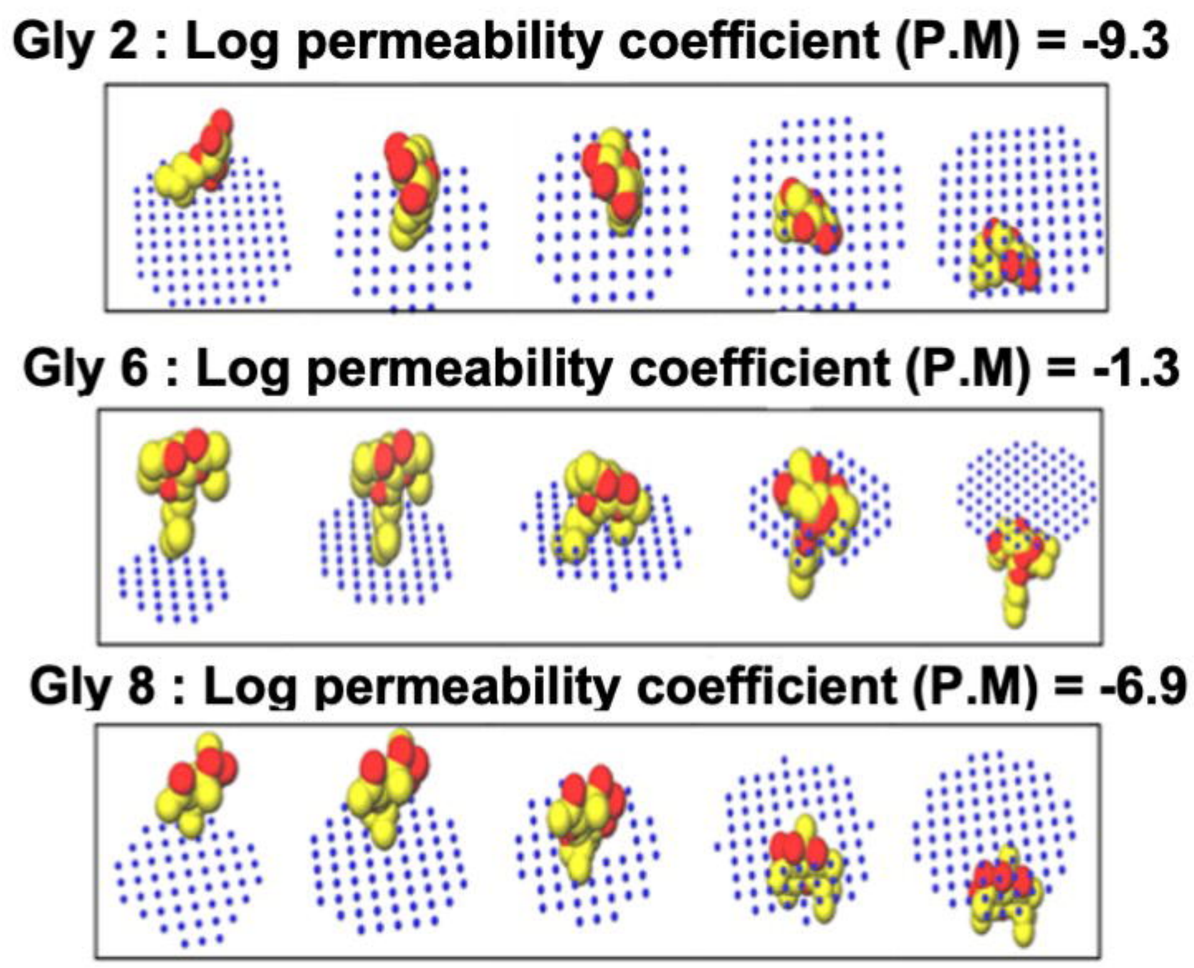

Figure. 2

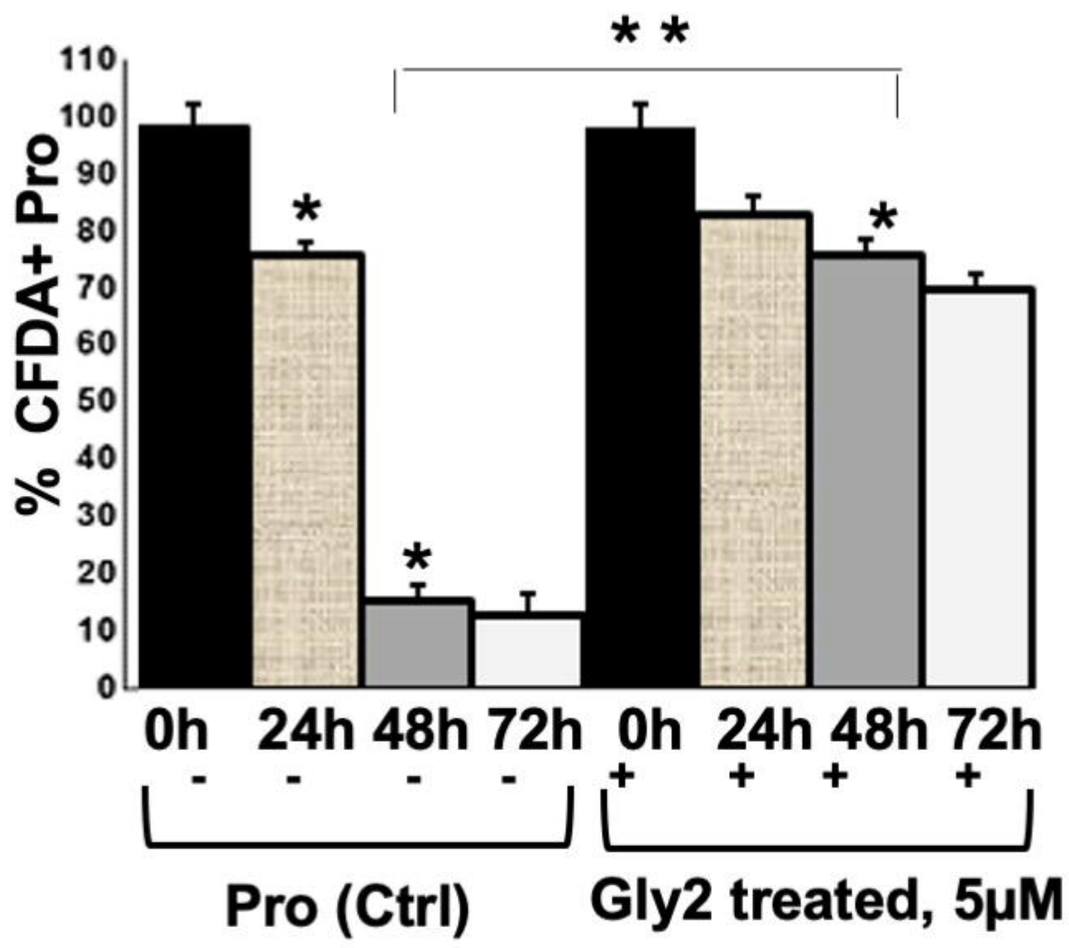
% CFDA+ Pro
110
100
90
80
70
60
50
40
30
20
10
0
* *
*
*
*
0h 24h 48h 72h 0h 24h 48h 72h
- - - - + + + +
Pro (Ctrl)
Gly2 treated, 5μM

Figure. 3

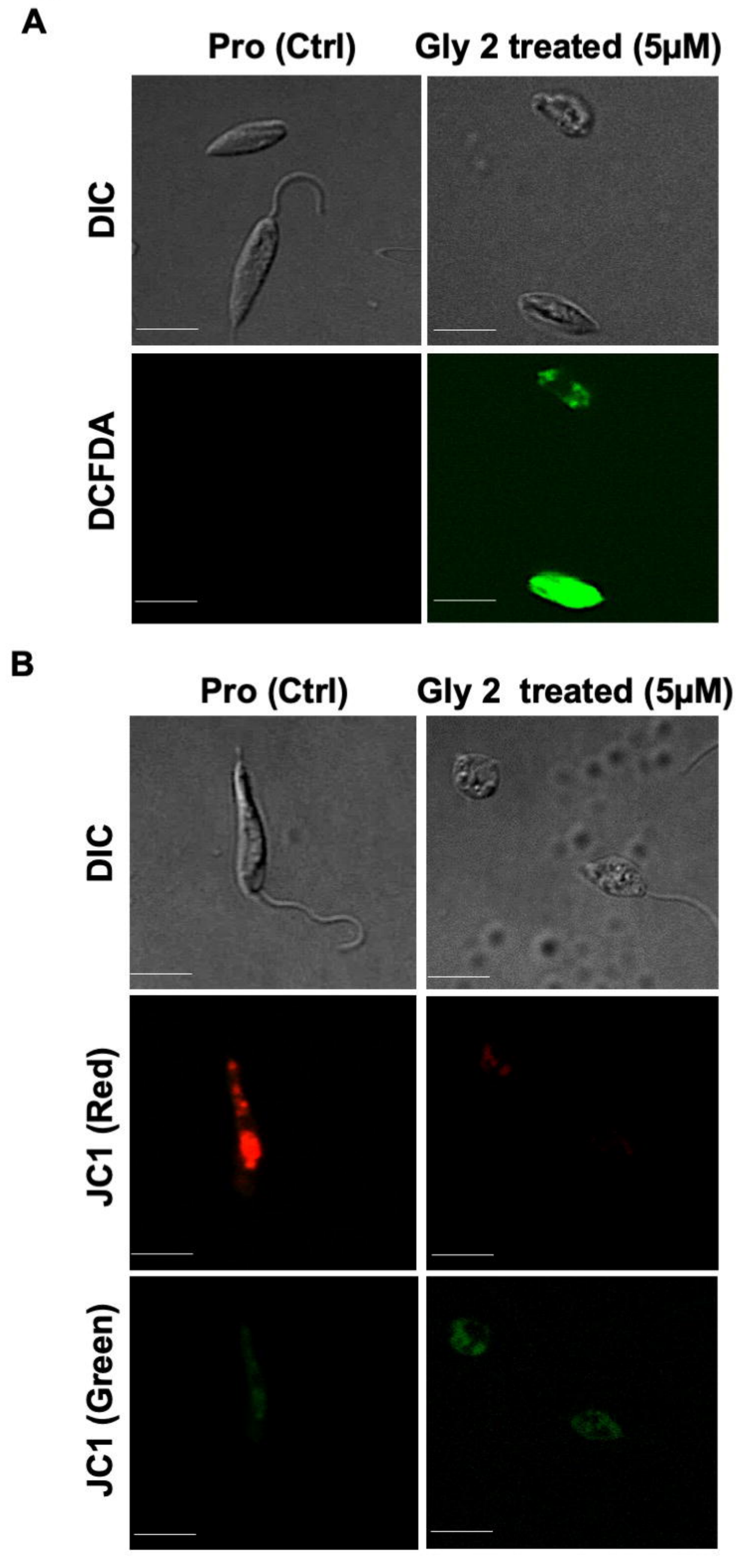
A
Pro (Ctrl)
Gly 2 treated (5μM)
DIC
DCFDA
B
Pro (Ctrl)
Gly 2 treated (5μM)
DIC
JC1 (Red)
JC1 (Green)

Figure. 4

A

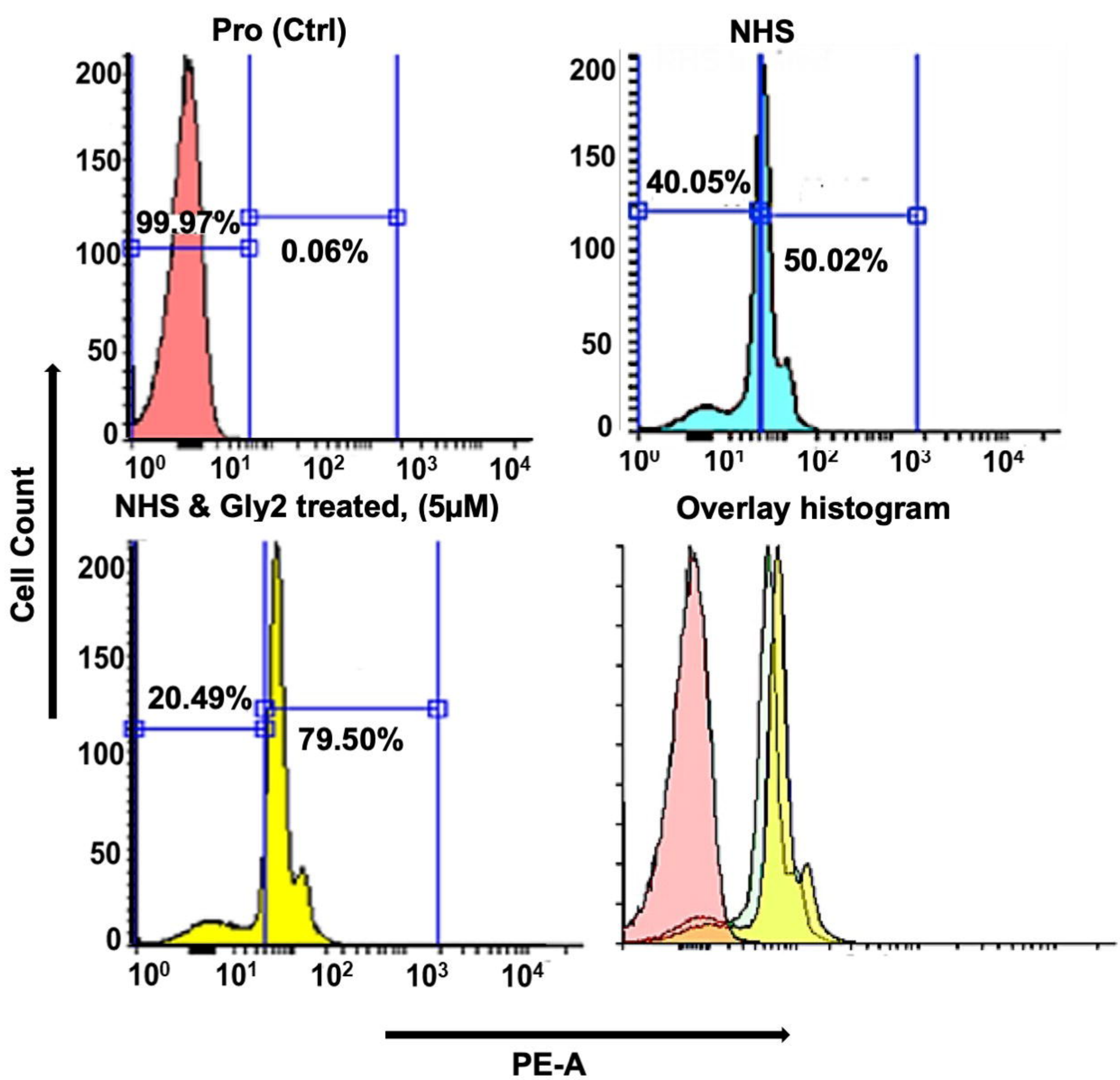
Pro (Ctrl)
NHS
99.97%
0.06%
40.05%
50.02%
NHS & Gly2 treated, (5μM)
Overlay histogram
20.49%
79.50%
Cell Count
PE-A

B

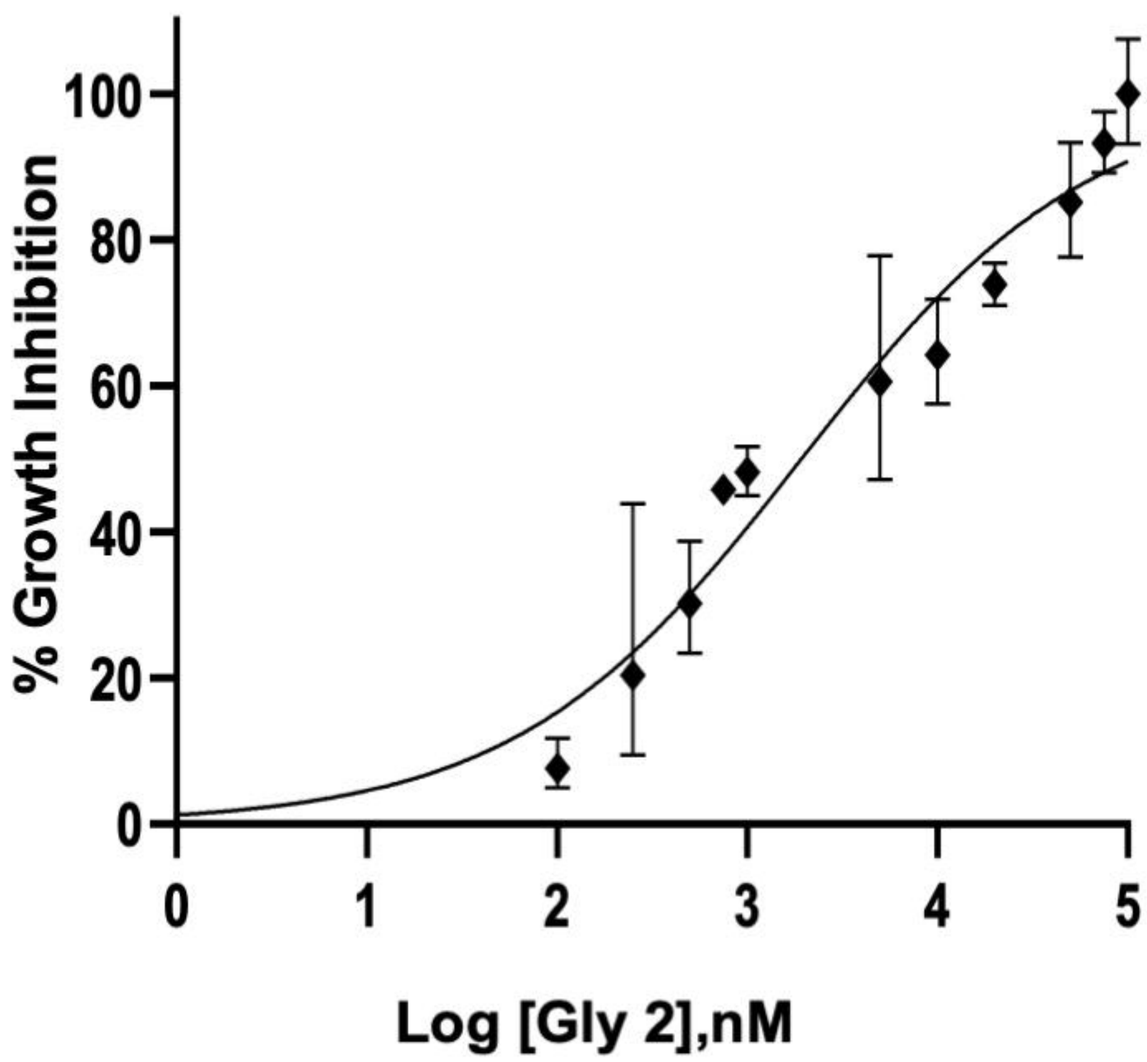
% Growth Inhibition
Log [Gly 2],nM

Figure. 5

A

Energy Minimized L.*donovani* Gp63

Estimated TM-score = 0.95
Estimated RMSD = 2.91

B

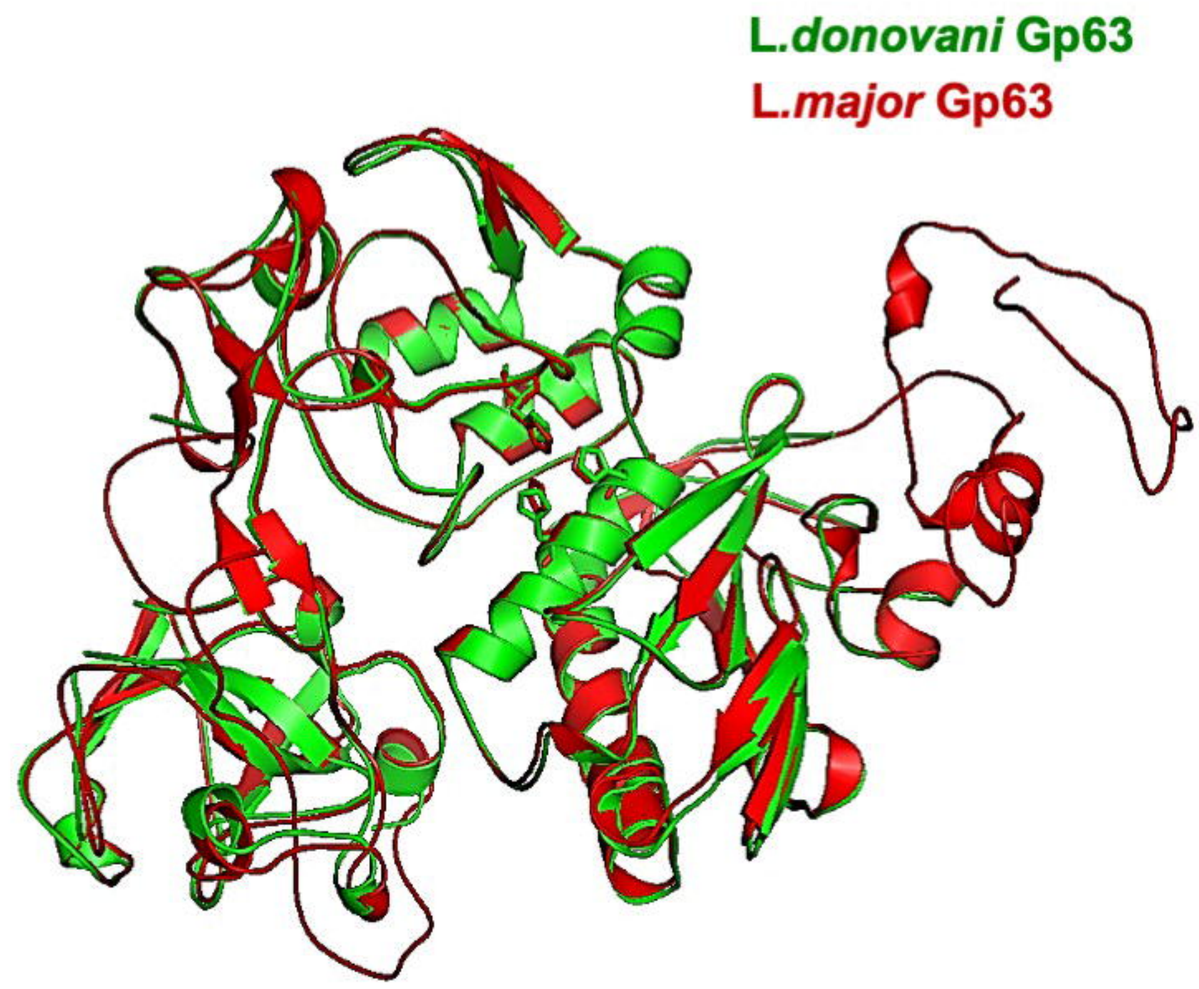

C

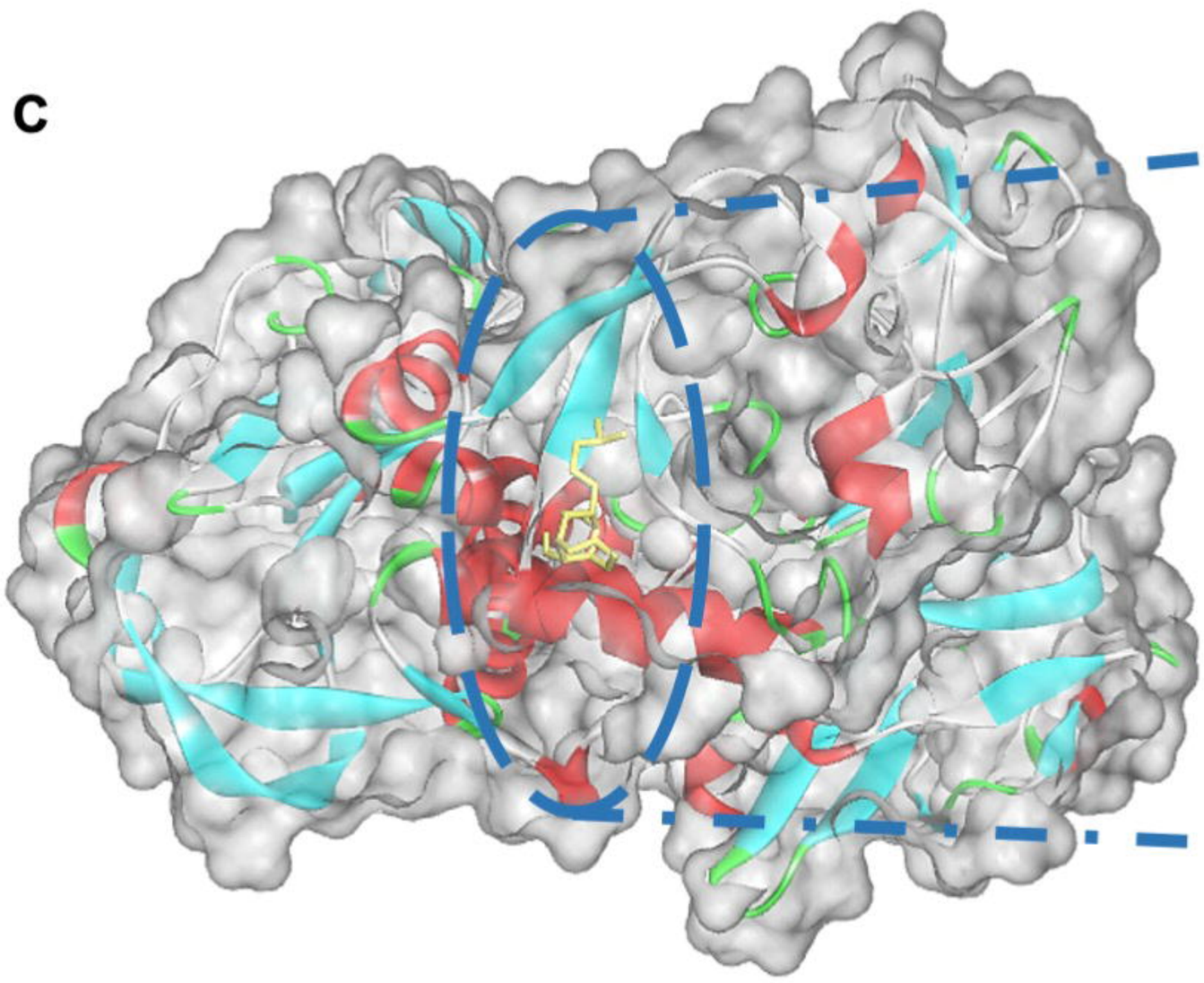

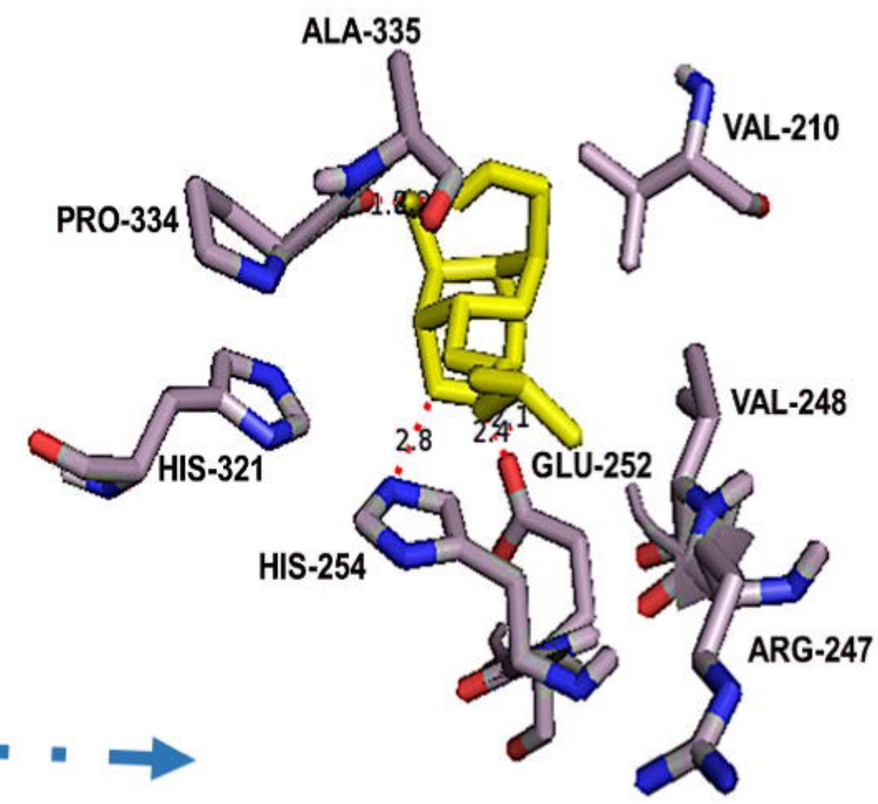

D

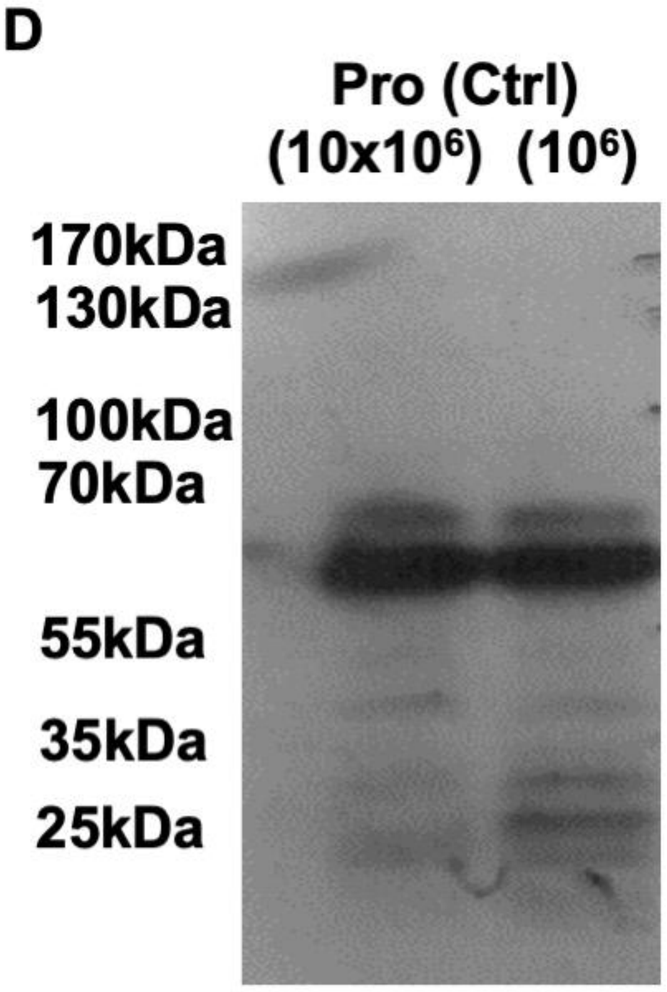
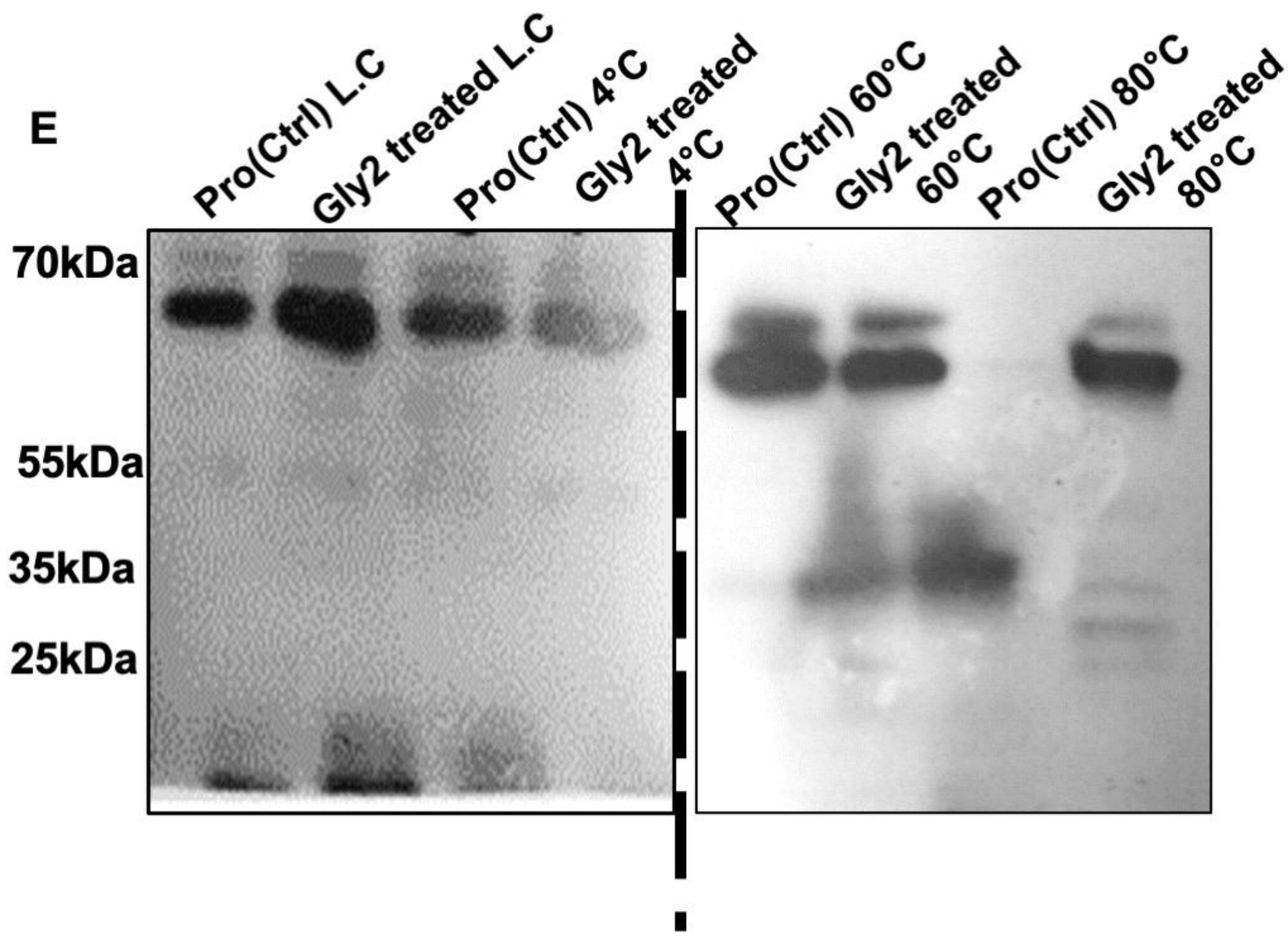
E